Journal of Materials Chemistry A

Accepted Manuscript

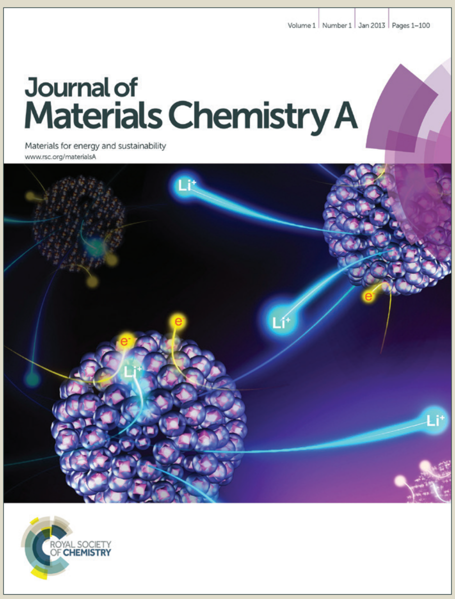

ROYAL SOCIETY OF CHEMISTRY

www.rsc.org/materialsA

Journal Name RSCPublishing

ARTICLE

Cite this: DOI: 10.1039/x0xx00000x

A Review on 'Self-cleaning and Multifunctional Materials'

Prathapan Ragesh,[a] V. Anand Ganesh,[b] Shantikumar V Nair[a] and A. Sreekumaran Nair*[a]

Received 00th January 2012,
Accepted 00th January 2012

DOI: 10.1039/x0xx00000x

www.rsc.org/

This review article exemplifies the importance of self-cleaning materials and coatings. Self-cleaning coatings are becoming an integral part of our daily life because of their utility in various applications such as windows, solar panels, cements, paints, etc. In this review, various categories of materials for the fabrication of hydrophilic, hydrophobic, oleophobic, amphiphobic and multifunctional coatings and their synthesis routes have been discussed. Furthermore, different natural organisms exhibiting superhydrophobic behaviour have been analysed. This review also covers the fundamentals of self-cleaning attributes such as water contact angle, surface energy, contact angle hysteresis, etc.

1 Introduction

Man mimics the kaleidoscopic forms of nature[1] and one such vivacious source is the self-cleaning surfaces (**Fig. 1**) inspired by the lotus leaf[2], legs of water strider[3], wings of cicada[4], gecko's feet[5], wings of butterflies[6], etc. Self-Cleaning coatings prove to be labour-saving technique due to their wide range of applications extending from glass coatings, cement and paints to textiles.[7,8] Many companies have commercialized several self-cleaning multi-functional products which can be used effectively in our daily life.[9,10]

Self-cleaning coatings are primarily categorized into hydrophobic and hydrophilic[7]; both clean the surfaces by the action of water. The former make the water droplets to slide and roll over the surfaces, thereby carrying the dirt away with them, while the latter use appropriate metal oxides to sheet the water that removes the dirt from the surface. In addition to the sheeting effect, metal oxides have an additional property of chemically breaking down complex dirt deposits by a sunlight-assisted cleaning mechanism – *Photocatalytic effect*.[11] The review vividly deals with the basics of self-cleaning phenomena inspired by nature followed by hydrophobic/superhydrophobic, photocatalysis-based hydrophilic/superhydrophilic self-cleaning materials. Furthermore, recent advancements in self-cleaning surfaces including oleophobic & amphiphobic surfaces and multifunctional coating materials have also been analysed and discussed.

2 Basics of self-cleaning

The chemical composition and the geometrical structure of solid surfaces govern the wettability.[12] The angle measured through the droplet at the intervention of three phases - solid, liquid and vapour, is referred as the water contact angle (WCA).[13] The contact angle is modelled using Young's equation as follows.[14]

$$\cos\theta_c = (\Upsilon_{SV}-\Upsilon_{SL})/ \Upsilon_{LV} \quad (1)$$

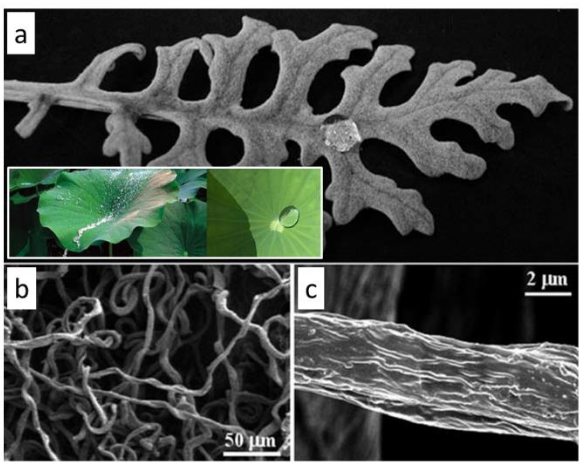

Fig. 1 Pictures of water droplets on Lotus (left) and Ramee (right) leaf indicating the self-cleaning property inherent in nature.[1] Inset of a: pictures of water droplet on Lotus (left) and Ramee leaf (right) indicating their inherent self-cleaning nature.

where ϒ represents the surface energy and SLV represents the solid, liquid and vapour phase, respectively. If the contact angle > 90°, the solid surface is referred as hydrophobic surface and if less than 90°, the surface becomes hydrophilic in nature. If the contact angle approaches more than 150°, the surface is termed as ultrahydrophobic/superhydrophobic surface. Similarly, as the contact angle approaches to 0° (water completely wets the surface), then the surface is termed as superhydrophillic surface (**Fig. 2**). David Quere studied the dynamic behaviour of droplets on ultraphobic surfaces whose findings are listed in a series of papers.[15-20] When the substrate is tilted to certain angle and the water droplets are made to move on such a tilted surface, the angle formed at the front of droplet motion is known as advancing angle θ_A and the rear angle is known as the receding angle, θ_R.[21] The differences between the advancing and receding angles gives

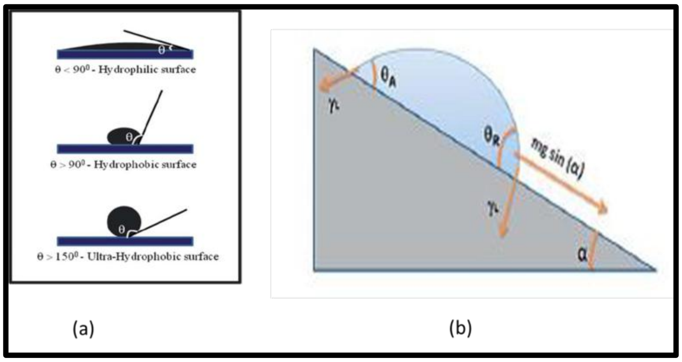

Fig. 2 (a) Schematic diagram indicating Hydrophilic, Hydrophobic and Ultra-Hydrophobic Surface and **(b)** Schematic representing water contact angle on a slanted surface.[23]

contact angle hysteresis value. The drops tend to stick onto the surface if contact angle hysteresis is too large[22] and hence low values of contact hysteresis angle and sliding angle are preferred which would help in the rolling down of the water droplets easily. Water contact angle is dependent on the surface roughness which is explained via two models: Cassie-Baxter[24] and Wenzel[25] (**Fig. 3**). Wenzel state reveals that the liquid keeps an intimate contact with a micro structured surface in which the change of contact angle is according to: [23]

$$\cos\theta_w = r\cos\theta \qquad (2)$$

where $\cos\theta_w$ is the Wenzel contact angle and *r* is the surface roughness factor. The water droplets penetrate into surface cavities and as a result of which the surface roughness factor tends to be greater than unity thus resulting in increase and decrease of contact angle for hydrophobic and hydrophilic surfaces, respectively. Cassie-Baxter model explains the heterogeneous wetting state in which water in the surface cavities entraps the air and as a result of which the liquid and solid interface area is minimized and that between water and air is maximized. This results in the formation of spherical droplets with lower hysteresis and the hysteresis could be further reduced by increasing the roughness (higher contact angle).[26] Both the models explains how surface roughness increases with increase in contact angle, but fails to explain the dynamic behaviour of moving droplets on a surface.[14] Above a certain roughness factor, Wenzel state transits to Cassie-Baxter model. It is vivid that biomimicing nature's phenomena is tedious and may result in several loopholes in the artificial design. For example, plants have the inherent ability to repair or rejuvenate them which may be an uphill task when trying to mimic as such. Even though self-cleaning surfaces like water-repellent fabrics have been fascinating objects in the market, still they are not ubiquitous. This is mostly due to the inefficacy of the as-such produced self-cleaning membranes to withstand high hydrostatic pressure and get easily damaged. Hence care must be given to produce practical surfaces which can withstand high pressures, have long durability and easy to manufacture. In totality it must be environmentally stable without any damage. Also the synthesized/fabricated self-cleaning membranes must be scratch resistant and must have good adhesion to the substrates on to which they are applied. No air gap should be present between the substrate and the coating applied. Because of the advantages over traditional coatings, cost-effectiveness and environmental friendliness, makes the nanostructured coatings witness great demand in industries including

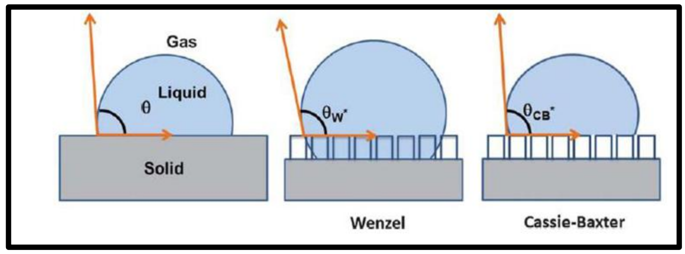

Fig. 3 Schematic diagram showing the water droplets on a flat solid surface, Wenzel model (middle) and Cassie-Baxter model (right).[27]

oil and gas, solar glasses, etc. Nanostructured materials have properties such as water-repellence, corrosion resistance, ultraviolet radiation stability, anti-microbial activity etc. which make them potential for various applications in day-to-day life.

3 Hydrophobic Surfaces

Due to a wide variety of applications such as in self-cleaning, stain-resistant fabrics, anti-corrosion, etc., hydrophobic surfaces tend to be a hotspot for researchers, a derivative of nature's marvellous phenomena.[28-36] Hydrophobicity is enhanced by the roughness factor.[37-46] The surface roughness is frequently controlled by the use of nanoparticles[47-54] which can be synthesized with uniform size and can be tuned via Stober method.[55] Fluorinated polymers are potential enough in creating hydrophobic materials with a static contact angle greater than 130°.[56] Such hydrophobic materials can be extensively viewed in the nature.[57] The electron micrographs in **Fig. 4** illustrate the ultraphobicity in two plant species highlighting the rough structure of leaves in microscale range. The Indian literature exemplifies lotus as the embodiment of purity which although originates from muddy water is devoid of dirt and other pollutants. This was first observed by Ward *et al.*[58] The leaf surface becomes superhydrophobic due to the presence of epicuticular wax crystalloids.

3.1 Mechanisms to produce Superhydrophobic Coatings

With tremendous applications of superhydrophobic surfaces, researches find interest in developing new technologies encompassed with a motto of low surface energy and controlled morphology on nano and micro scales. Broadly, the techniques to produce superhydrophobic surfaces can be categorized as: a) roughening of low surface energy materials; b) modification of rough surface with low surface energy materials.

3.1.1 Modifying a low surface energy material

Khorasani *et al.*[59] used CO_2 pulsed laser as an excitation source to modify PDMS(Polydimethylsiloxane) by introducing peroxide groups onto PDMS surface (**Fig. 5a and b**) which graft 2-hydroxyethyl methacrylate (HEMA) onto PDMS. The resulting contact angle was obtained as 175°. Porosity and chain ordering on PDMS surface resulted in such an increment in WCA. Jin *et al.*[60] induced roughness on PDMS surface using laser etching and obtained a WCA of 160°. Electrospinning technique was employed by Ma *et al.*[61] in producing superhydrophobic membranes. PS-PDMS/PS homopolymer (**Fig. 6**) exhibited a WCA of 163°. Such an increment in WCA is seen due to the ability of PDMS to enrich fiber surfaces and surface roughness with small fiber diameter. Due to low surface energy, fluorinated polymers are of great interest, which when roughened results in superhydrophobic surfaces. Zhang *et al.*[62] observed that when Teflon (polytetrafluoroethylene) was stretched, the superhydrophobicity was achieved, attributed by the presence of void space and fibrous crystals on the surface. Shiu *et al.*[63] observed that oxygen plasma treatment on Teflon yielded a rough surface with a WCA of 168°. However fluorinated materials are linked with rough materials in producing superhydrophobic surfaces rather than using it directly due to its limited solubility. Inexpensive superhydrophobic coating was produced by Lu *et al.* [64] using "low-density polyethylene" (LDPE), which yielded a WCA of 170°. Materials like alkylketene,[65] polycarbonate[66] and polyamide[67] are potential candidates exhibiting

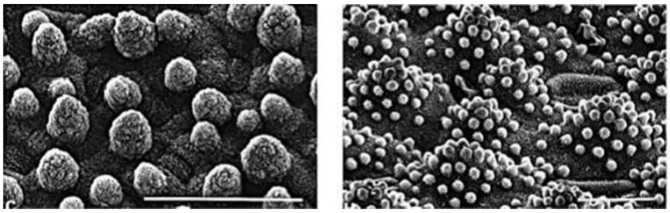

Fig. 4 Electron micrographs of ultraphobic leaves, Nelumbo nucifera (with a scale bar of 50 μm) in left and Hygoryza aristata (with a scale bar of 20 μm) in right, highlighting various textures.[57]

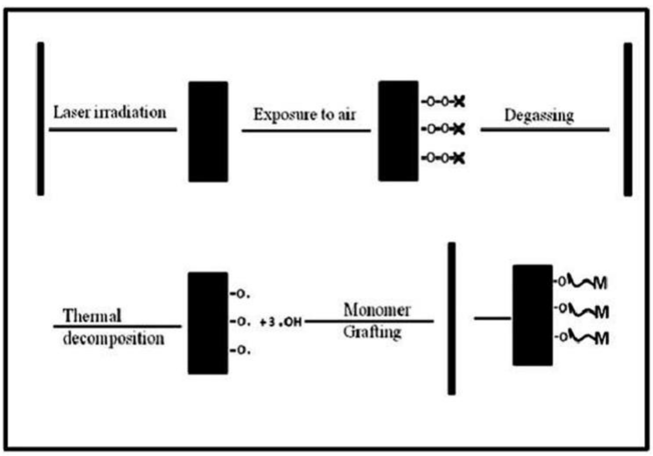

(a)

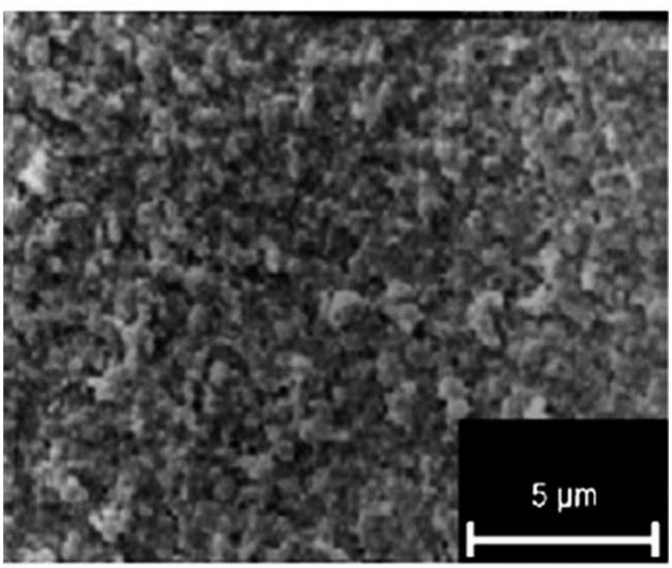

(b)

Fig. 5 (a) Schematic diagram depicting laser induced graft polymerization technique[59]. **(b)** SEM image showing the treatment of CO_2 pulsed laser on PDMS surface.[59]

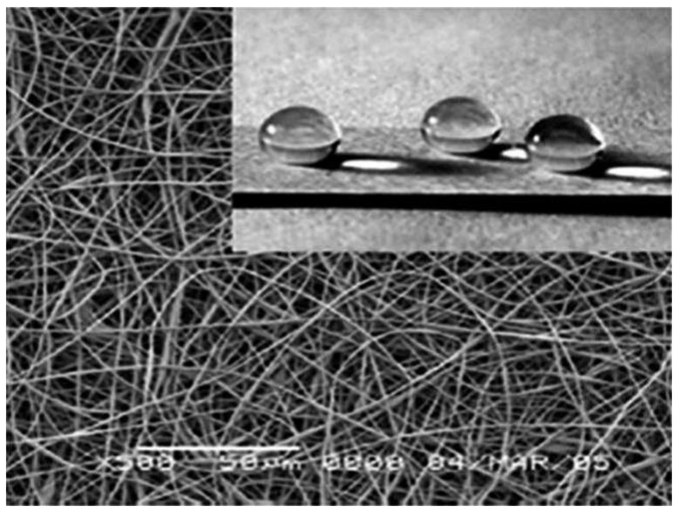

Fig. 6 SEM image of droplets on PS-PDMS/PS electrospun mat.[61]

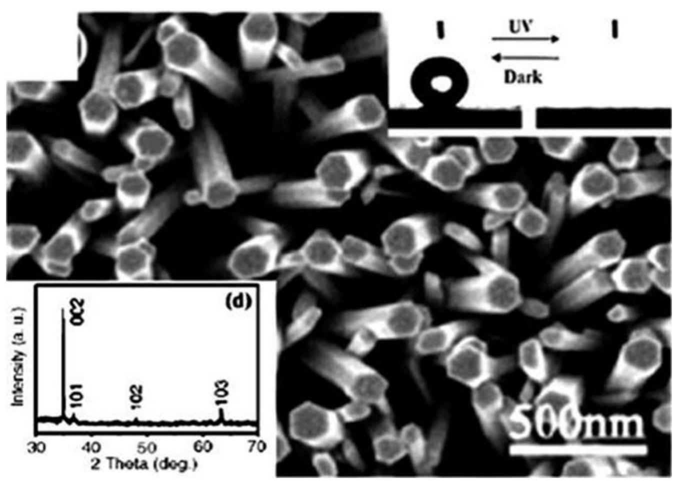

Fig. 7 SEM image of aligned ZnO nanorods synthesized by two-step solution approach.[68]

superhydrophobic properties. ZnO nanorods were synthesized by Feng *et al.*[68] using a two-step solution method (**Fig. 7**). Due to low surface energy of (001) plane, ZnO nanorod films turned out to be superhydrophobic, but when exposed to UV light turns to be superhydrophilic because of adsorption of hydroxyl group on its surface.

3.1.2 Synthesizing a rough surface and modifying it with a low-surface energy material

Controlled dimensionality and morphology of nanostructures like nanowires, nanoparticles etc. were obtained using wet chemical reactions.[69,70,71] Superhydrophobic surface on copper substrate was produced by chemical method by Jiang *et al.*[72] Superhydrophobicity was attained through surface modification of substrate by immersing the substrate into n-tetradecanoic acid solution for about a week. Wet chemical process was utilized to create superhyrophobic surfaces on nickel substrates in which monoalkyl phosphonic acid reacts with Ni producing flowery microstructures.[73] Another efficient bottom up route is hydrothermal technique by which we can fabricate functional materials with different patterns and technologies.[74-77] In situ hydrothermal synthesis was employed to create nanolamellate

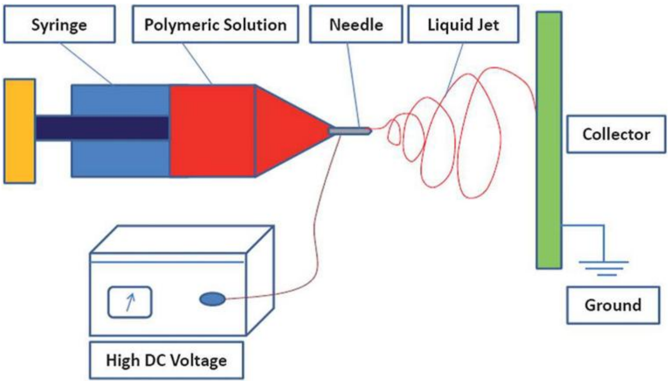

Fig. 8 A schematic representation of Electrospinning procedure.[14]

structures on titanium.[78] Through surface modification using PDMSVT, the superhydrophilic surface was converted to superhydrophobic surface. Biomimetic superhydrophobic surfaces were synthesized using electrochemical deposition, a versatile technique for producing microscale and nanoscale structures.[79-84] Galvanic deposition technique on metals was employed by Bell *et al.*[85] to deposit metallic salt solution resulting in the formation of superhydrophobic surface with a WCA of 173°. Lithography techniques such as photolithography, electron-beam lithography, X-ray lithography, etc were employed to create micro and nanopatterns.[86-95] Photocatalytic lithography technique was utilized on composite surfaces by Notsu *et al.*[96] to synthesize superhydrophilic and superhydrophobic patterns. Inexpensive techniques like self-assembly and layer-by-layer (LBL) were employed for the formation of multilayer thin films with controlled surface morphologies.[97-109] Rambutan-like surface with hollow spheres of aniline was fabricated by Jiang *et al.*[97] using self-assembly technique. Assembly of silica particles was done by Lee *et al.*[104] to obtain raspberry-like particles with dual-size surface roughness. A versatile technique to produce nanofibres is electrospinning which enhances the surface roughness and produces continuous nanofibres. A hydrophobic material when electrospun results in superhydrophobicity.[110] Micro and nano surface patterns could be produced on macroscopic substrate.[111-113] using chemical vapor deposition process (CVD). Some of the other techniques that are used for making superhydrophobic surfaces include sol-gel method (all kinds of solid substrates[114-121] could be used), polymerization technique,[122-125] texturing,[126,127] electrospraying,[128,129] sandblasting,[130] etc.

3.1.2.1 Hydrothermal technique

Hydrothermal technique is an efficient technique for creating nanostructures under high pressure and temperature conditions. It is an environmentally benign technique and can be used for low temperature processing (T < 200 °C, P < 1.5 MPa).[131-133] No additional calcination and grinding or milling of the initial mixture is required which makes it cost-effective. The size and shape of the nanoparticles formed can be controlled by controlling the synthesis temperature, concentrations of the precursors, etc.[134] Typically hydrothermal technique works on the principle of temperature gradient method. The nutrient solution is taken in the jar and is heated to create two zonal areas- hot and cold zone. The nutrient dissolves in the hotter zone and when it gets saturated in the lower part, it is made to move towards the upper part by the convective motion. During

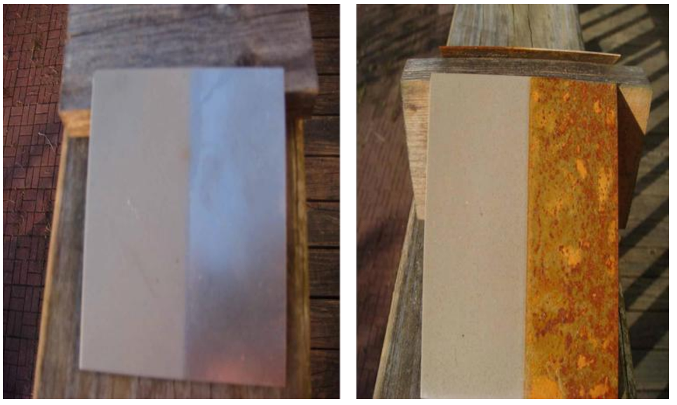

Fig. 9 Photographs depicting coated (left) and non-coated (right) steel plates taken after exposure to atmosphere for about 60 days (adapted from www.ornl.gov/File%20Library/.../06-Superhydrophobic_Materials.pdf).

this time, the cooler upper solution descends to the hotter zone and by reducing the temperature of the upper part, supersaturation is initiated for crystallization process. The parameters governing the process are temperature, pressure, pH of the solution and duration of synthesis. If pH > 8, more OH^- ions tend to move to the surfaces and passivate the high surface energy plane and the growth happens thereafter to yield elongated structures like nanowires, nanorods etc. If pH < 4, spiroidal shapes are observed.

3.1.2.2 Electrospinning Technique

With the development of nanotechnology, electrospinning has got importance in producing continuous nanofibres with high surface roughness. Basically an electrospinning set-up consists of a high-voltage supply, a grounded collector, syringe loaded with precursor solution and a pump for regulating the flow of the precursor solution (**Fig. 8**). When the high voltage applied at the tip of the syringe exceeds the surface tension of the precursor solution, a Taylor cone is produced first which then forms a jet. For the Taylor cone[136] formation, the applied voltage must exceed a critical voltage[137] given by the equation below:

$$V_c = \sqrt{\frac{\gamma H^2}{r\varepsilon}} \tag{3}$$

where Vc indicates the critical voltage, γ refers to the surface tension of the precursor solution, H refers to the distance between the needle tip and the collector, r is the radius of meniscus and ε refers to the permittivity. The jet being unstable gets accumulated at the collector surface where the fibres are obtained. The parameters governing electrospinning are: surface tension of the precursor solution, concentration of the precursor solution, viscosity of the precursor solution, the applied voltage, flow rate of solution, and distance between the tip of syringe and collector. If the viscosity of the solution is high, there are high chances of clogging and if it is low, electrospraying happens instead of electrospinning. The bead formation in the resulting fibres could be controlled by optimizing the viscosity of the solution. For electrospinning to happen, sufficient voltage (5-30 kV) needs to be applied, else results in spraying. The distance parameter is critical as it has to be optimized to facilitate the evaporation of the solvent before the collection of fibres on the collector. Nowadays, humidity controllable electrospinning set-up is available which remedies the bead formation in the resulting fibres.

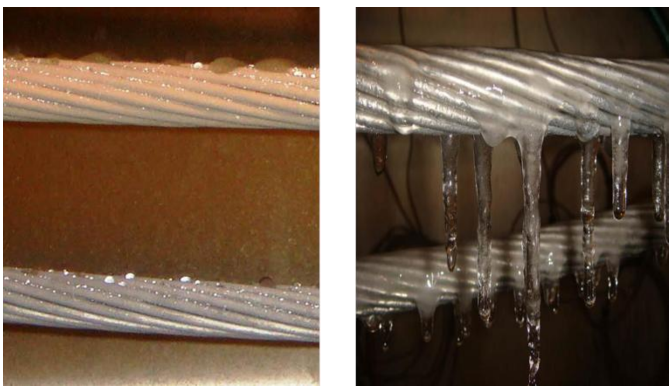

Fig. 10 Photographs of coated (left) and uncoated cables (right) depicting the functionality of hydrophobic coatings for anti-icing (adapted from www.ornl.gov/File%20Library/.../06-Superhydrophobic_Materials.pdf).

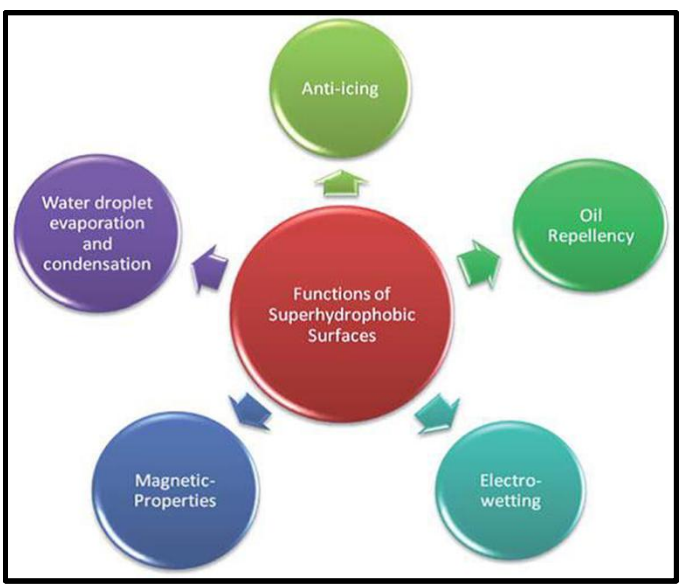

Fig. 11 Pictorial representation of application areas of hydrophobic surfaces.[1]

Hydrophobic surfaces find plenty of applications like anti-corrosive systems (**Fig. 9**), anti-icing (**Fig. 10**), water repellence, etc. In industry, it is widely used for ultra-dry and surface applications. On applying the coating, air molecules comes in contact between the coating and the substrate, thus increasing the WCA. Superhydrophobic coatings enhance the fuel efficiency in maritime industry by reducing the skin friction drags occurring in ship hulls. Such a coating increases the ship speed and also acts as anti-corrosive systems, preventing any organic contaminant or marine microorganisms to come in contact with the ship hulls. In vehicles, superhydrophobic coatings are applied on the glasses to prevent them from clinging, thereby helps in cleaning the car thyself. Also such superhydrophobic membranes are used in water desalination plants for effective fresh water generation. A well-known superhydrophobic coating used in small boats is "HullKote speed polish", which gives surface protection on boats and is easy to use. In medical field, superhydrophobic coatings when applied to the medical instruments provide sterility by detaching the bacteria from the instrument surface. Cao *et al.*[138] investigated the utility of superhydrophobic coatings for anti-icing and found that such treated surfaces prevent ice formation by inhibiting the frost nucleation process. Anti-icing capability also depends upon the size of the particles exposed on the surface. The factors affecting the frost nucleation were studied in detail by Na *et al.*[139] Formation of ice depends on several other factors like temperature, surface roughness, contact area etc. Intensive research is still ongoing in this field which will be a boon for mainly colder regions of the world. Another interesting phenomenon found with superhydrophobic surfaces is electrowetting behavior. Krupenkin *et al.*[140a] demonstrated the change of wettability from a superhydrophobic state to complete wetting state as a function of tuning voltage and liquid surface tension (**Fig. 12**).

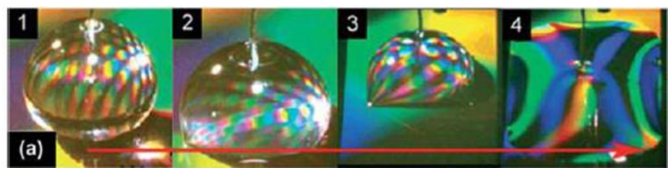

Fig. 12 Electrowetting behavior of liquid by tuning the voltage and surface tension.[140]

Anti-bacterial textile encompassing superhydrophobicity was developed by Ivanova et al.[140b] for biomedical applications. Nanoparticle (NP) dispersion was sprayed over textile sample for the coating formulation which resulted in multiscale textured layer on the top of cotton fabric. Chitosan-based NPs incorporated anti-bacterial functionality to the coating. Electrostatic interaction between amine group of Chitosan and negatively charged fluoroanion was used as the basis for the nanoparticle fabrication. It was observed that the structure of aggregates in the coating and wettability and durability of coating is regulated or controlled by the relative number of fluoroanions/elementary unit of chitosan. Shateri-Khalilabad et al.[140c] fabricated superhydrophobic and electroconductive textiles using graphene-coated cotton cellulose. Dip-pad dry method was used to deposit graphene oxide on cotton fibres followed by reduction with ascorbic acid which yielded graphene-layer incorporated fabric. Poly methylsiloxane (PMS)

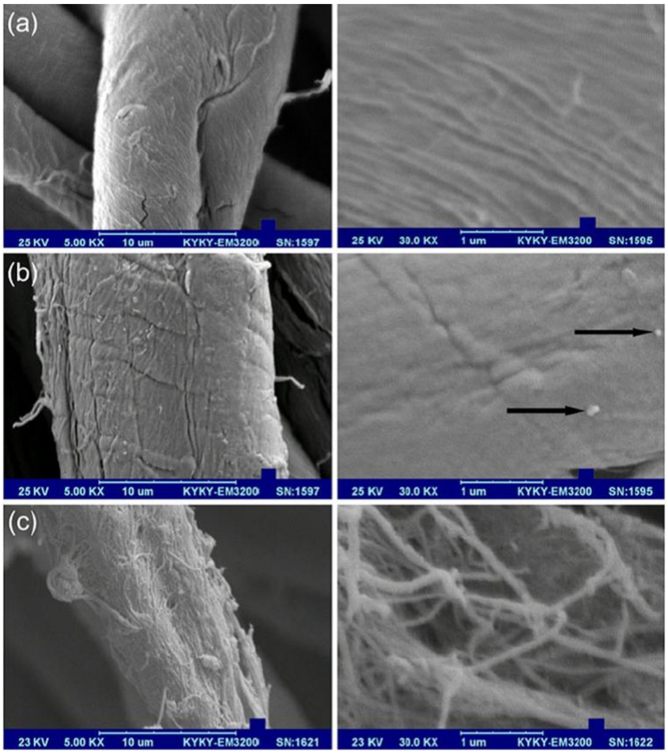

Fig. 13 (a, b and c) SEM images of original cotton, graphene- cotton and PMS-graphene-cotton respectively with the right hand side showing its higher magnification images.[140c]

nanofilaments were formed on the fiber surface by the reaction of fabric with methyl trichlorosilane. Such fabric (**Fig. 13**) coated with graphene showed hydrophobicity with a contact angle of 143.2°±2.9°. The self-cleaning ability of the fabric consisting of PMS nanofilaments was evident from a contact angle of 163°±3.4° (superhydrophobic character).

Wang et al.[140d] fabricated superhydrophobic asymmetric cotton fabrics (**Fig. 14**) using graft-polymerization process with atomized lauryl methacrylate as monomer. Nanoscale hierarchical structures are formed on the cotton surface using the synthesized polymers. By choosing a suitable solvent or by varying the monomer mist stream, the surface morphology could be controlled. An asymmetric superhydrophobic surface was obtained by surface modification of cotton fabrics without any additional nanosized particles. Modified cotton fabric has laundering durability and mechanical stability with a water contact angle more than 150° revealing its superhydrophobic character.

Inspired from mussel adhesion, Zhu et al.[140e] fabricated superhydrophobic surfaces and a one-step and versatile strategy for the robust immobilization of oxides nanoparticles. By tuning the pH or adding n-dodecanethiol, the oxidation of dopamine could be tuned which internally have a great influence on the immobilization of the nanoparticles. Effective oil separation from water surface through a magnetic-actuated manner was done using the superhydrophobic PU sponges and exhibited highest space utilizations for oil-storage.

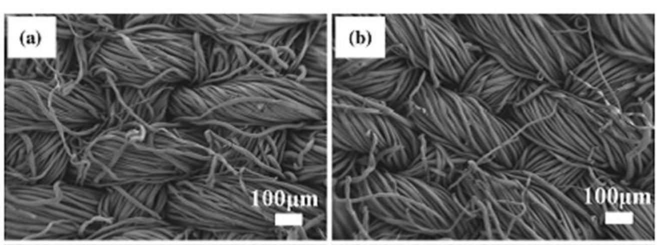

Fig. 14 SEM images (low magnification) of a) pristine cotton fabric and b) cotton fabric modified with mist-polymerization process.[140d]

4. Hydrophilic Surfaces

Irrespective of potential applications of hydrophobic surfaces (**Fig. 11**), researchers also focus on hydrophilic surfaces that proved to be useful in water purification, paint industry, etc. These clean the surfaces by the process of photocatalysis followed by sheeting of water. The wettability of such surfaces is normally high as a result of which the water contact angle tends to be approximately 0°. In spite of such a cleaning ability, it is still in a matured state compared to the hydrophobic coatings and research is still going in this field to innovate an efficient cleaning capability for such coatings by varying the material compositions.

4.1 Photocatalysis

Pilkington[7] was successful in commercializing the first self-cleaning windows in 2001. Following them, several other companies came forward in the same area. These windows utilized titanium-dioxide (TiO_2) as transparent coatings, by which the cleaning happens in two distinct ways: photocatalysis, a process in which the organic dirt molecules get decomposed in the presence of sunlight and the sheeting of water which makes the surface superhydrophilic (contact angle ~ 0°) thereby carrying away the dirt molecules. TiO_2 has become a potential candidate exhibiting photocatalytic activity and it is widely used because of its non-toxicity, availability, cost effectiveness, chemical stability, favourable physical and chemical properties etc. TiO_2 is used even in paint and cosmetics as pigment and as a food-additive. The material is also used in anti-pollution applications, water-purification (the membrane is coated with TiO_2 that kills the bacteria present in water), etc. Several forms of TiO_2 are available among which the primary phases are: anatase, rutile and brookite phase. The most common form of TiO_2 is the rutile phase which is densely packed and is used in pigments as sun-blockers and paints. The anatase phase is rare and has open crystal structure which makes it highly photocatalytic. Both anatase and rutile phases have tetragonal structure. The brookite phase, being orthorhombic is extremely rare. Anatase phase TiO_2 when heated to more than 400 °C becomes rutile phase. Photocatalysis can be generally categorized into two classes of processes. The process in which the adsorbate molecule being photoexcited interacts with the ground state catalyst substrate is known as a catalyzed *photoreaction*.[141] Instead, if the initial photoexcitation takes place in the catalyst substrate and transfers an electron or energy into a ground state molecule, the process is referred to as a *sensitized photoreaction*.[141] The quantum yield (number of events occurring per photon absorbed) determines the efficiency of a photocatalytic process. By analyzing all the possible pathways for electrons and holes, the efficiency or quantum yield is calculated. TiO_2 being a semiconductor, upon absorption of light greater than or equal to its band-gap, gets excited to produce electrons and holes. Most of these charge carriers undergo recombination and some migrate to the surface. The electrons produced move from valence band to the conduction band where it react with the atmospheric oxygen to produce superoxide radicals. These

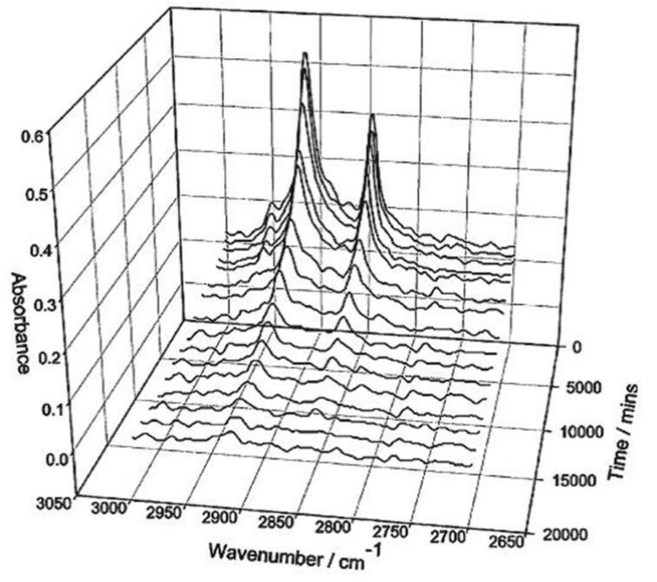

Fig. 15 Stearic acid undergoing photocatalytic decomposition, monitored by infrared spectroscopy.[142]

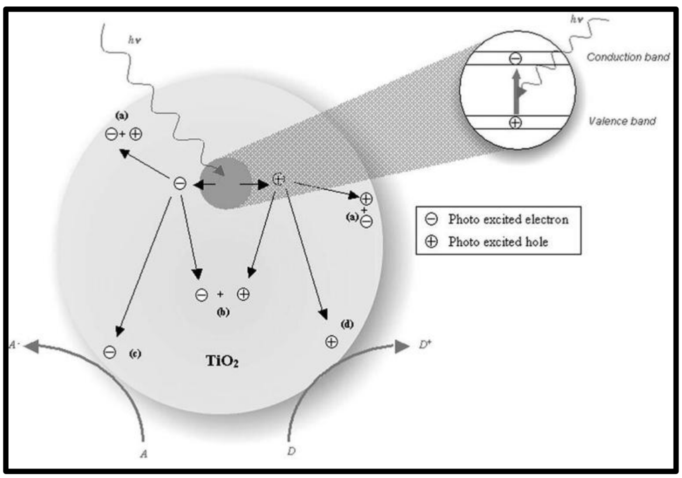

Fig. 16 Schematic representation of different processes occurring when Titanium-dioxide absorbs ultra-band-gap light.[7]

superoxide radicals, being highly energetic decompose the organic dirt into carbon-dioxide and water, a process referred to as the *cold combustion process*. The decomposition of stearic acid into carbon-dioxide and water vapour in the presence of atmospheric oxygen occurs on a TiO_2 surface, leaving behind no by-products (**Fig. 15**), thus proving to be a remarkably clean surface.[142] The destruction of a modelled pollutant is done to analyze the photocatalytic property of a material. The popular choices of such modelled pollutants include stearic acid, methylene blue, chlorophenol, etc. The holes produced in the valence band oxidize the surface oxygen producing oxygen vacancies, onto which the hydroxyl radicals are adsorbed (sheeting of water). This lowers the contact angle ~ 0°, thus making the surface superhydrophilic in nature. Thus the band-gap of TiO_2 and the electron-hole generation (**Fig. 16**), both together control the self-cleaning property. The advancement in nanotechnology with the use of nanoparticles, nanowires, nanotubes, nanoflowers, etc. typically in the range of 1-100 nm has brought a great pace in making nanoscale TiO_2 with

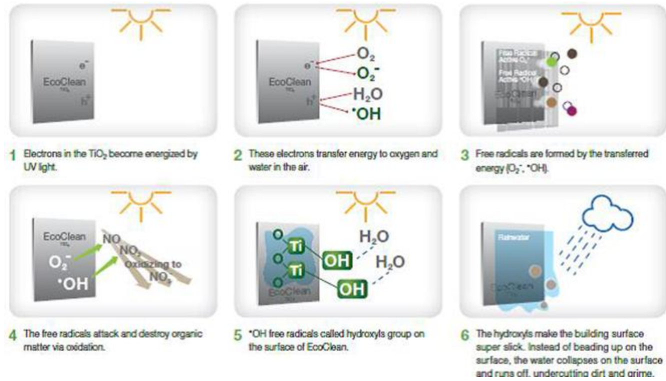

Fig. 17 Various steps in photocatalysis achieved using the Titanium dioxide coating on the buildings (Pre-painted Aluminium surfaces).[144b]

increased photocatalytic effect because of its large surface to volume ratio and a wider band-gap, thereby oxidizing and reducing holes and electrons, respectively to a great extent than the bulk TiO_2.[143] Still there are a lot of challenges that need to be overcome by nanocrystalline TiO_2 especially its robustness and optical transparency in glazing industries. For enhanced coatings, some strategies may be employed like increasing the lifetime of charge carriers by reducing the recombination, increasing the absorption of light to longer wavelengths thereby extending to larger area of solar spectrum, increasing the number of charge carriers and surface area of the film deposited, etc. It is indicated that thicker films when deposited increases the number of excited charge carriers by absorbing more light. But nevertheless above 25 nm, it is seen that there is a wide chance of recombination because of the thick film which makes the charge carriers difficult to move towards the surface. Also more the thickness, more the cost per unit area because of longer deposition time and the amount of material required and also sacrifices the optical transparency and durability, thus hindering the thicker films to be used for window coating applications. Another brilliant approach in enhancing the self-cleaning property of TiO_2 is doping in which the impurities added influence the photocatalytic activity of TiO_2 even in low concentrations. In this scenario, wide transition metals as dopants have been reported based on their oxidative powers.

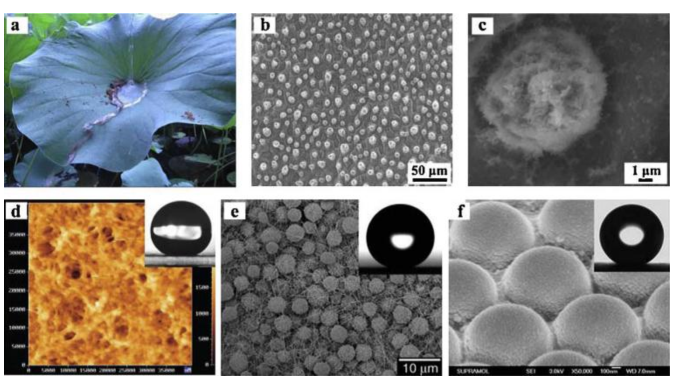

Fig. 18 **(a)** Demonstration of self-cleaning effect in which the dirt particles are carried away by the rolling water droplets. **(b)** SEM image (low magnification) showing random micropapillae structures in lotus effect. **(c)** Cilium –like nanostructures superimposed on the top of micropapllae observed in the SEM image of a single papilla. **(d)** AFM image of a i-PP coating. Insite shows a water contact angle of 160° measured via water droplet on the coating applied on a glass slide.[152] **(e)** Special microsphere/ nanofiber composite structures observed in SEM image of polystyrene films (superhydrophobic) synthesized via EHD

technique.[153] **(f)** Ag nanoparticles composite arrays observed in SEM image of biomimic surfaces. Inset shows water contact angle of 166°.[151]

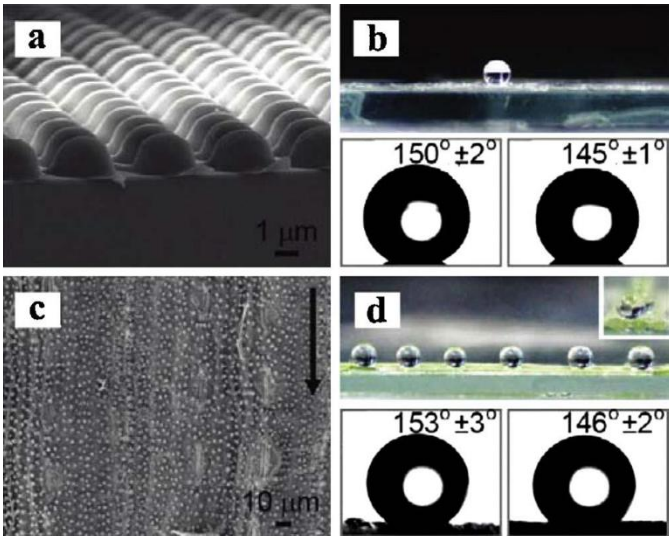

Fig. 19 Figures exemplifying the similarity between anisotropic surfaces and natural rice leaf. **(a)** micropearl arrays SEM image (cross-sectional). **(b)** Upper photo shows the modified micropearl arrays with water droplet. The lower figure shows the contact angle measurement of fluoroalkylsilane modified surface. **(c)** Structures clearly seen in SEM image of natural rice leaf. **(d)** Digital photos buttressing the similarity of designed anisotropy to those with natural one.[158]

The photocatalytic activity of transition metal cations like Fe^{3+}-, Co^{2+}- and Ni^{2+}- doped TiO_2 are low compared to the transition metals with higher oxidation states such as Mo^{5+}, Nb^{5+}, W^{6+}, etc. High proportion of hydroxyl groups are adsorbed on to the surface of high oxidation state transition metal surfaces compared to the lower oxidation transition metal surfaces, which was confirmed using X-ray photoelectron spectroscopy (XPS). This clearly explains why higher oxidation state metal dopants increase the photocatalytic behavior when added to TiO_2, thus enhancing superhydrophilicity. Several other materials than TiO_2 have been investigated for self-cleaning (superhydrophilicity) such as CdS, WO_3, ZnO etc., but none has become successful in surpassing the efficacy of TiO_2 till now.[144a,145a] Alcoa Architectural products[144b] introduced an innovative coating comprising of TiO_2 that helps in making the buildings clean themselves. They coat a TiO_2 layer to a pre-painted aluminium surface, thus washing away the contaminants in presence of Sun. The details of the cleaning action achieved could be seen in **Fig. 17**. Titan Shield TM Solar Coat[145b] uses TiO_2 as a photocatalyst material (inexpensive coating technique in which the TiO_2 is sprayed to the desired substrate, mainly of glass) for photovoltaic panels to provide better transmittance and lower reflectance, thereby increasing the efficiency of the solar panel using superhydrophilicity. Because of the superhydrophilic nature, the treated glass surface becomes devoid of water droplets thus rendering the surface clean during rain.

5. Natures Contribution

5.1 Lotus leaf

Nelumbo nucifera (the lotus plant) is considered to be an embodiment of purity in Asian religions. The dirt-resistant property of lotus leaf has made the researchers to investigate its miracle effect in detail. Randomly distributed micro-papillae of about 5-9 µm in diameter enclosed by fine nanostructured branches of 120 nm in diameter was observed (**Fig. 18b and Fig. 18c**). The presence of such surface structures and epicuticular wax crystalloids made its surface highly superhydrophobic with small sliding angles. Thus the dirt particles are carried away by the rolling spherical water droplets, an intrinsic process called self-cleaning or lotus effect (**Fig. 18a**). Several researchers have investigated in biomimicing this lotus effect to create artificial superhydrophobic surfaces.[146-150] whose water contact angle is greater than 150° (**Fig. 18d**). Recently flexible superhydrophobic films were synthesized on flexible hemisphere arrays by thermal evaporation of Ag nanoparticles. The deposited film was then modified with 1-dodecanethiol.[151] It was found that the obtained morphology had resemblance with the natural micro/nano structures present in lotus leaf (**Fig. 18f**). Using electrohydrodynamic technique, polystyrene film with superhydrophobic nature was synthesized that had porous microspheres and nanofibers (**Fig. 18e**).

5.2 Rice leaves

Hierarchical structured papillae are arranged in quasi-one-dimensional order similar to those of lotus leaf. Such special structures make the rice leaf both superhydrophobic and impose anisotropic wettability, thereby the water droplets roll easily along the direction parallel to the rice leaf. Carbon nanotube film of rice-like alignment was prepared by surface deposition of catalyst in a controlled manner so as to mimic the anisotropic wetting function of rice leaf.[154] Au surfaces with positive and negative textures were fabricated to biomimic rice leaf textures in which rice leaves were used as templates.[155] Anisotropic micro/nanoscale hierarchical structures were observed on Au surface indicating anisotropic sliding angle performances. Reduction of adhesion between water droplets and the surface (with negative texture) was observed when the surface was modified with 1-decanethiol. Two-step phase-separation micro-molding process was investigated recently to replicate rice leaf structures.[156] The artificial structures thus replicated showed similarity to the natural rice leaf structure with anisotropic wetting. When the replicated artificial structures were modified or treated with poly (N-isopropylacrylamide), they showed good thermal responsive wettability.[157] Laser interference lithography technique was proposed to achieve controlled anisotropic wetting through which large area micropearl arrays were fabricated.[158] It was found that there exists similarity between natural rice leaf and anisotropic wettability of biomimetic materials which is illustrated in **Fig. 19**.

5.3 Butterfly wings and peacock feather

The scintillating colors present in wings of butterfly charm everybody and thus have attracted many researchers like Hooke, Newton etc. to do research. These mind capturing colors are a result of structural color (iridescence) and pigmentation.[159] The interaction of light with complex architectures results in so-called structural color. Multiscale photonic structures ranging from nanometer to millimeter that are found on wing scales, imparts brilliant blue iridescent colors for Morpho butterfly (found in Central and South America).[160-162] The multiscale structures in addition to the brilliant iridescent color imparts superhydrophobicity and acute chemical sensing ability to the butterfly wings. The scales present in wings can be categorized into two types[163]: the structural color is due to ground scales and superhydrophobicity

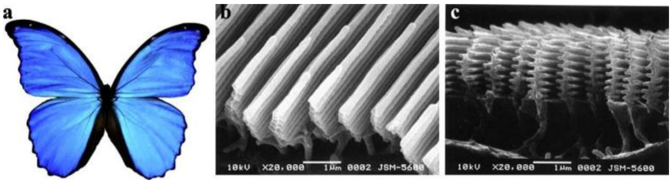

Fig. 20 (a) Morpho butterfly. **(b)** Oblique view SEM image. **(c)** SEM image indicating the ground scale of Morpho butterfly.[168]

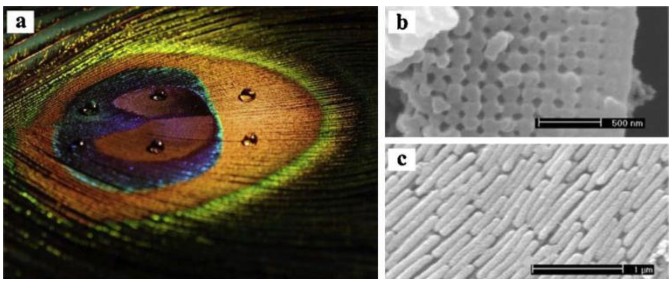

Fig. 21 (a) Peacock feather showing superhydrophobicity. **(b** and **c)** SEM images of barbule structures.[167]

and self-cleaning properties are due to cover scales. One-dimensional oriented arrangement with directional adhesion was observed in Morpho butterfly wings.[164] Lamella-stacking nano-stripes covering micro squamas overlap the above oriented arrangement. It was observed that water rolls easily along radial outward direction but gets tightly pinned in opposite direction. Scientists being inspired with such multiscale structures of butterfly design biomimetic materials for functional integration. Self-assembly of polystyrene spheres and silica nanoparticles was done to fabricate a uniform opal film, mimicking Morpho butterfly wings (**Fig. 20**). The film exhibited superhydrophobicity[165] with structural colors. Alumina coating through a low-temperature atomic layer deposition (ALD) process was done to replicate micro and nanometer scale hierarchical photonic structures with natural butterfly wings as the templates.[166]

Another natural material with structured color is peacock feather. The peacock feather displays iridescent colors and intricate eye patterns in the tails (observed in male peacock).

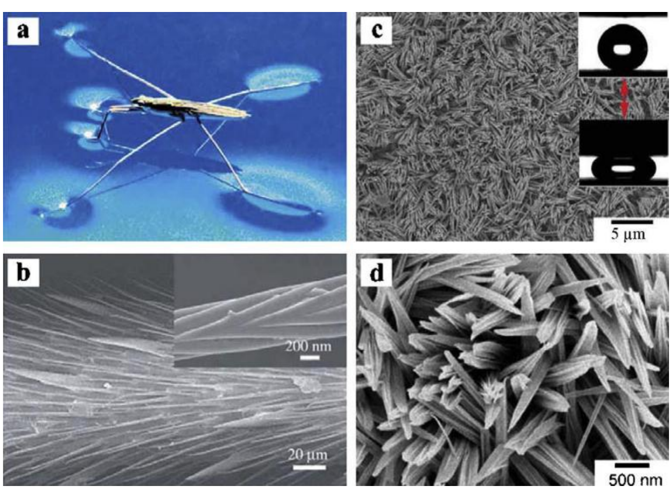

Fig 22 (a) Photograph depicting a water strider signifying its superhydrophobic nature **(b)** SEM image of leg **(c)** Low and **(d)** High magnification SEM image exemplifying the Copper hydroxide nanoneedle arrays.[187]

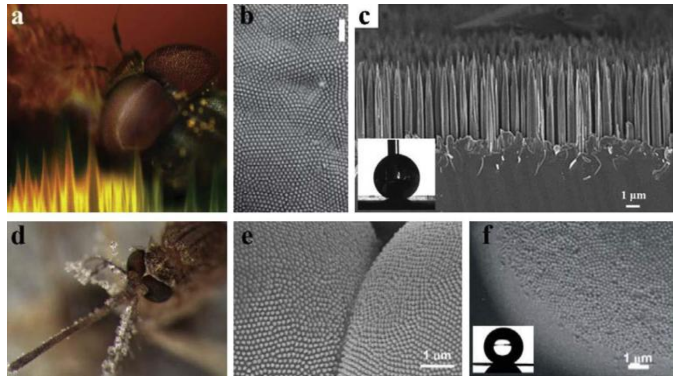

Fig. 23 (a) Compound eyes of Moth. **(b)** Figure showing the SEM image of a moth eye with anti-reflective surface. **(c)** SEM image (Cross-sectional view) of silicon hollow-tip arrays. **(d)** Image highlighting the mosquito eyes after exposure to water aerosol. (e) SEM image showing adjacent ommatidia. **(f)** SEM image exemplifying the analogue between artificial compound eye and a water droplet (spherical) on a surface.[187]

The kaleidoscopic color production in peacock (Pavo muticus) feathers (**Fig. 21**) is due to tiny two-dimensional photonic crystal structure.[167] In addition to color, superhydrophobicity is also observed in peacock feather. The variation in the colour is attributed to the change in lattice constant and the number of periods in photonic crystal structure.

5.4 Water strider legs and Insect compound eyes

Water strider (Gerris remigis) effortlessly moves on water using its legs.[169] Researchers trying to mimic its legs found that water strider's leg (**Fig. 22**) was covered with needle-shaped micrometer scale setae with a surface inclination of 20°. Numerous helical nano-grooves were found to in each microseta which traps even tiny air bubbles.[170] Apart from all these features, water strider's legs were found to have a hydrophobic character. Until a depth of 4.3 mm is covered, water strider's legs do not pierce the water. Because of the tremendous support offered from its leg, water strider is flexible even under turbulent conditions in moving water. A water volume of about 300 times of its leg is flushed off exemplifying its hydrophobic nature. Inspired from water strider's leg, a superhydrophobic robust copper surface was fabricated that comprised nanoneedle arrays embedded with nanogrooves.[171]

Anti-reflective surfaces are found in some insects that impart attractive properties.[172-174] For instance, the eyes of moth (**Fig. 23**), butterfly and fly has anti-reflection and attractive physiological optics in high sensitivity due to the presence of multiscale structure.[175-178] The insects's head consists of a compound eye that again is an aggregation of several little eyes known as ommatidia. Several multifunctional artificial compound eyes have been designed to biomimic such eye structures with antireflective properties. The suppression of reflection of light at a range of wavelengths from Ultraviolet to terahertz region was observed in silicon nanotips that were arranged as aperiodic arrays.[179] Such structures find immense applications in renewable energy sector especially photovoltaic devices. Metal catalytic wet etching of silicon was employed in fabricating high aspect ratio silicon hollow tip arrays that biomimiced moth compound eye.[180] These arrays possessed high anti-reflective properties along with hydrophobicity. Recently, silica substrates were used to construct superhydrophilic surfaces along with anti-reflective and anti-fogging properties. The presence of surface multiscale structures comprising hexagonally non-close-packed nano-nipples covering micro-ommatidia was observed in the compound eyes of mosquito. Soft lithography technique was used to create artificial compound eye with superhydrophobicity and anti-fogging properties that mimic mosquito compound eyes.[181] Anti-reflection property is also found in insect wings for camouflage. Superhydrophobic anti-reflective self-cleaning properties were found in the wings of cicada.[182-184] Self-cleaning and anti-reflective properties were combined to form so called *multifunctional optical coatings*.[185,186] Such coatings are used in glass modules for photovoltaic applications so as to enhance its efficiency by repelling the dust and dirt molecules and transmitting almost all the light incident on it.

6. Oleophobic Surfaces

Oleophobic surfaces are oil-repelling surfaces. Such surfaces find immense applications in steel, oil and marine where oil spilling results in havoc. Choi *et al.*[188] investigated oleophobicity using a dip-coating process on various surfaces with inherent re-entrant texture. Tunable wettability along with reversible-deformation dependent property was observed in such dip-coated fabrics. Also such surfaces have shown high wetting properties with various polar and non-polar liquids. Researchers try to fabricate various superhydrophobic/superoleophobic surfaces by biomimicing nature. Oleophobic surfaces have immense capability for self-cleaning and anti-fouling characteristics. In order to synthesize a superoleophobic surface (oil and organic liquids have lower surface tension), the solid surface in air must have a surface energy lesser than oil. Chae *et al.*[189] studied the wetting behavior of water and oil droplets at three-phase interfaces for oleophobic surfaces. A material with a low surface energy compared to oil was used for fabricating oleophobic surfaces at solid/air/oil interface with various contact angles of oil and water droplets. Surface energies at different interfaces were studied to understand oleophobicity applications in the underwater regime. Contact angles of water and oil was predicted using a model which was validated by studying the wetting behavior of micro-patterns and flat surfaces (with changing pitch value). Wang *et al.*[190] engineered superoleophobic surfaces on functional titanium using a novel anodization method or its combination with laser technology approach. TiO_2 nanotube arrays were formed on a microstructured titanium surface after which hydrophobic materials were post-modified. By applying varying UV and annealing, switchable wettability was achieved towards superoleophobicity. Also reversible adhesion of oil droplets between sliding and sticky superoleophobicity was achieved. Such engineered surfaces were accounted for their applications in oil sealing and anti-creeping. Aulin *et al.*[191] demonstrated the formation of structured porous aerogels (using freeze-drying) which was comprised of NanoFibrillated Cellulose (NFC). FE-SEM and nitrogen adsorption/desorption measurements indicate high porosity of aerogels and their low density (<0.03 g/cm^3). Tuning of surface texture and density was done by appropriate selection of NFC dispersion concentration before freeze-drying. The aerogel was uniformly coated so as to tune their wetting properties towards non-polar liquids. This was done using Chemical Vapor Deposition of 1H,1H,2H,2H-perfluorodecyltrichlorosilane (PFOTS). A robust composite interface was observed for modified aerogels with an apparent contact angle of $\theta >> 90°$ for castor oil and hexadecane. By Solid-Liquid-Vapor composite interface generation and trapping microscopic air pockets, realization of surfaces having strong wetting to oil and low surface tension liquids can be made. Such a composite interface is metastable for liquids with low surface tension such as hexadecane (γ_{lv} = 27.5 mN/m) which is attributed by the lower value of equilibrium contact angle. As a result, metastable composite interface gets converted fully to wetted interface irreversibly due to pressure perturbations. Chhatre *et al.*[192] investigated tuning the liquid wettability of polyester fabrics using thermal annealing procedure and dip-coating technique. The fabric surface was uniformly coated with a mixture of 90% polyethyl methacrylate (PEMA) and 10% 1H,1H,2H,2H-heptadeca fluorodecyl polyhedral oligomeric silsesquioxane (fluorodecyl POSS). High contact angle values were achieved for robust metastable surfaces like hexadecane (γ_{lv} = 27.5 mN/m) and dodecane (γ_{lv} = 25.3 mN/m). A reversible treatment in contact with dry air/water using thermal annealing was carried out to tune the solid surface energy of coated surface. Reversible switchable oleophobicity between a highly non-wetting and fully wetted surface was achieved for hexadecane and dodecane (low-surface tension liquids) by tuning the solid surface energy attributed by polyester fabric with inherent re-entrant texture. For liquids with lower surface energies than water, a contact angle greater than 150° was displayed by superoleophobic surfaces. Geometrical shape of etched silicon surfaces on the contact angle and hysteresis observed when surface comes in contact with different liquids needs to be apprehended for the design of superoleophobic surfaces. Liu *et al.*[193] created superoleophobic surfaces on Si (111) surface using various silane treatments and liquid-based metal-assisted etching technique. The oleophobicity of Si (111) was controlled by the concentration of the etch solution and duration of etching. When different silane treatments were applied to the silicon surface, a transition from Cassie to Wenzel state (for low-surface energy liquids) was observed from apparent contact angle. A relation between the contact angle transition among Cassie and Wenzel behavior on etched Si (111) surfaces and the re-entrant angle of etched surface structures were observed. Bellanger *et al.*[194] investigated the synthesis and characterization of 3-4-ethylene dioxy pyrrole derivatives having two fluorinated tails. Elaboration of superoleophobic surfaces was achieved using such monomers by electrodeposition of conducting polymers. The presence of two fluorinated chains exhibited high steric hindrances during electro-polymerization which was evident from Cyclic Voltammetry experiments. Various deposition methods were employed to enhance surface oleophobicity. Galvanostatic deposition technique and pulse potentiostatic deposition technique was employed to create superoleophobic surfaces with contact angle approximately 140° using PEDOP. The presence of surface microstructures and nanoporosites were the reason responsible for superoleophobic property. Dong *et al.*[195] investigated water and oil wettabilities of silica surfaces modified with hierarchical POSS. A mono substituted FPOSS (fluorinated POSS) was synthesized and silica particles were decorated with POSS nanocages by one-pot reaction. This was done to biomimic the lotus leaf thereby achieving self-cleaning property. It was observed that the surface after modifying with fluorinated copolymer shown high oil-repellency. Hydrophobic and oleophobic coatings constituting ceramic particles such as SiO_2, SiO, Al_2O_3 etc. with thermal and chemical durability were developed as an alternative to Teflon. Using spin-coating method, these coatings were applied on aluminium substrates.[196a] Superoleophobic surfaces were fabricated via perfluorothiolate reaction which was carried out on nanostructured $Cu(OH)_2$ surfaces. Such surfaces showed controlled oil adhesion and finds immense application for oil transportation[196b]. By adjusting external preload forces and surfaces nanostructures, the surface adhesion to oil could be controlled, thereby making it fit for oil transportation in a safer way (**Fig. 24**). Oil droplet-based microreactor for oil transportation was constructed using superoleophobic surfaces. Hydrophobic-oleophobic properties were observed in high-thermal resistant heteroatomic polymers like polyimides when modified by the addition of fluoro oligomers. It was observed that such coatings exhibited excellent scratch resistance and was harder than coatings devoid of ceramic particles. Steele *et al*.[197a] fabricated superoleophobic coatings using spray casting of nanoparticle-polymer suspensions. ZnO nanoparticles blended with a perfluoroacrylic polymer emulsion (water borne) were employed in this method using co-solvents. Acetone was found to be a potential co-solvent in producing self-assembling nanocomposite slurries. The speciality of such coatings was that no additional surface treatments were required as the nanocomposites were inherently superoleophobic. Tuteja *et a*l.[197b] fabricated a superoleophobic surface by the usage of re-entrant surface curvature in the surface design in conjunction with chemical composition and roughened texture. Such surfaces displayed high repellency to several low surface tension liquids including alkanes. For the fabrication of surfaces with re-entrant curvature, two different approaches were utilized. In each case, the non-wetting behaviour was exhibited in accordance with the Cassie state. Recently, for various polar liquids, silicone nanofilaments were used to fabricate superoleophobic coatings via a grow-from approach which yielded ultralow sliding angles for the surfaces[198a]. During TCMS (trichloromethylsilane) hydrolysis and condensation, regulation of water concentration in toluene is done so as to monitor the surface microstructure and oleophobicity. Such superoleophobic coatings exhibited excellent environmental and chemical stability along with good anti-reflection property. Anti-reflective property was shown during fabrication of silicone nanofilaments at low concentration of water. This resulted in an increment of

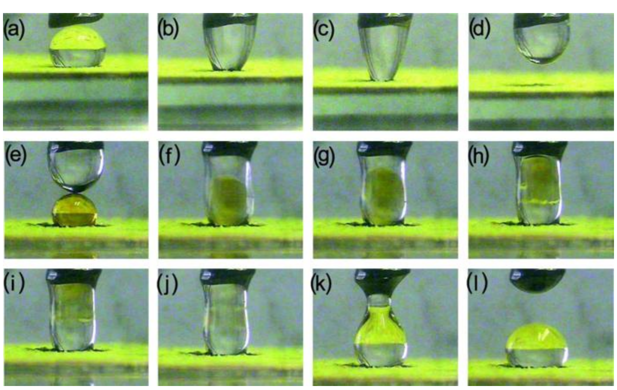

Fig. 24 Images indicating the proof of superoleophobic surfaces used in oil based microreactor. To transport oil droplets, a metal cap is used and superoleophobic surfaces with different oil adhesion are used as substrate. (a-d) Low adhesive superoleophobic surface transporting oil droplets to the metal cap; (e-f) oil droplet(with different chemicals-styrene and Br_2) getting coalesced; (g-j) In oil based microreactor, due to the reaction between the different chemicals in oil, the colour fades; (k-l) Due to high adhesion the final droplet is left on the substrate.[196b]

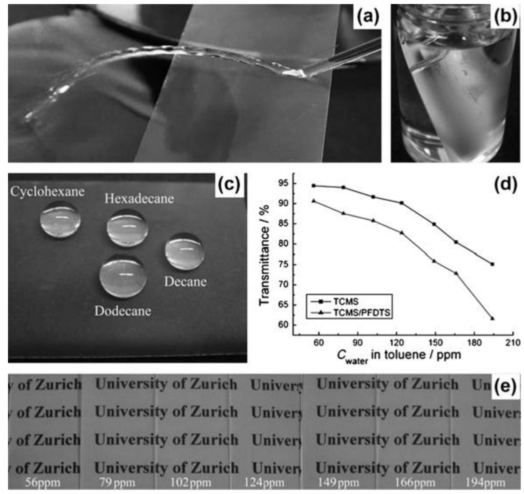

Fig. 25 Images of glass slides coated with TCMS/PFDTS (a) toluene jet bouncing off; (b) glass slides in toluene; (c) glass slides with various droplets of nonpolar liquids; (d) Graph indicating the enhancement of transmittance with TCMS/PFDTS; (e) Image showing the text upon which the TCMS/PFDTS coated glasses are kept.[198a]

transmittance from 91.2% (bare glass) to 94% at 600 nm (**Fig. 25**). A slight decrement in transmission was observed after modification with PFDTS (perfluorooctyl/perfluorodecyl trichlorosilane). The nanofilaments present in the surface decreased the light scattering thereby maintaining good transparency.

Li et al.[198c] reported nanometer-thick polymer coated surfaces which are more wettable to water than to oil and indicated their cause due to combination of nanoscale and interfacial phenomena which are kinetic in nature. The key factor to the specific size of the intermolecular hole in the polymer layer is due to the interaction between nanometer-thick polymer and substrate, which in turn determines the penetration kinetics of water and hexadecane. The peculiar wetting performance is observed when the hole size is appropriate such that hexadecane has much slower penetration rate than water. Cheng et al.[198d] fabricated surfaces with controlled underwater oil wettability by self-assembly of mixed thiols ((containing both $HS(CH_2)_9CH_3$ and $HS(CH_2)_{11}OH$)) on nanostructured copper substrates. Switchable underwater superoleophilicity to superoleophobicity for surfaces with controlled oil wettability is achieved by changing the concentration of $HS(CH_2)_{11}OH$ in the solution. The synergistic effect of nanostructures and surface chemistry variation on the surfaces could be the reason for the tunable effect discussed above. Also selective oil-water separation on as-prepared copper mesh films was realized.

7. Amphiphobic coatings

Amphiphobic coatings repel both water and oil. In-short, it is a combination of hydrophobicity and oleophobicity. Ganesh *et al.*[198b] fabricated a stable superamphiphobic coating using electrospinning technique on glass substrate with rice-shaped TiO_2 nano/mesostructures (**Fig. 26**). It was observed that the as-such fabricated TiO_2 nanostructures were superhydrophilic in nature, but turned to be superamphiphobic upon salinization. The obtained WCA (**Fig. 27)** were 166° and 138.5° using water (Surface tension γ =72.1 mN/m) and hexadecane (Surface tension γ= 27.5 mN/m), respectively. A contact angle hysteresis of 2° and 12° was obtained for water droplet and hexadecane. Thus a thermally and mechanically stable, cost-effective coating with better adherence to glass surface was fabricated. Lee *et al*.[199] used nanotransfer molding and controlled etching of the facile undercut to fabricate a nanoscale re-entrant curvature possessing superhydrophobic and superoleophobic surfaces. Such a method prevents capillary-induced bundling effects because of the ordered re-entrant nanostructures. Water droplet bouncing and contact angle measurements were done to demonstrate superhydrophobic and superoleophobic characteristics. Xiong *et al*.[200] used bifunctional silica particles and epoxy glue bearing poly(2-perfluorooctylethyl methacrylate) (PFOEMA) and poly(acrylic acid) (PAA) coronal chains to fabricate amphiphobic particulate coatings. A rough particulate coating was obtained by spraying particles comprising both PAA and PFOEMA (dispersed in trifluoro toluene) onto a glass plate containing epoxy film. Using a two-step mediated sol-gel technique, amphiphobic organic-inorganic hybrid coating materials were prepared by Nagappan *et al*.[201] First step included hydrosilylation reaction with polymethyl hydrosiloxane and 2,2,3,4,4,4 hexafluorobutyl methacrylate. The reaction was carried out for the synthesis of fluorinated polymethyl hydrosiloxane (precursor) in which Pt was used as the catalyst. The reaction of precursor and tetraethyl orthosilicate was carried out in the second step to prepare fluorinated polymethylsiloxane/silica hybrid (FSH) in which equivalent amount of water and varied quantities of ethanol were used. The reaction was carried out at a temperature of 70-80 °C for 24h. Sheen et al.[202] fabricated superamphiphobic coating material using fluorinated silica nanoparticles. The contact angle measurements gave a value of 167.5° and 158.6° for water and diiodomethane, respectively. A higher water contact angle was also observed for soyabean oil (146.6°), decahysronaphthalene (142.5°), xylene (140.5°) and diesel fuel (140.4°). The as-such developed coatings repel both water and organic liquids. Plasma modification of benzoxazine films **(Fig. 28)** were carried out by Wang *et al*.[203] to fabricate super-amphiphobic surfaces. During the plasma treatment process, a micro/nano binary structure is formed with rugged surface by fluorination and microroughening of benzoxazine films. High advancing contact angles of 157° and 152° were obtained for water and diiodomethane, respectively due to the effect of substrate roughness and low surface energy. Also low contact angle hysteresis was observed for such surfaces. (Fluoroalkyl) silane (FAS) modification of electrospun pure silica nanofibrous mats were carried out by Guo *et al*.[204] for fabricating amphiphobic mats which were found to be flexible and highly heat–resistant. A solution of poly(vinyl alcohol) (PVA) and silica gel were blended and was electrospun to obtain inorganic silica nanofibrous mats. In order to remove the organic component, the obtained mat was calcinated. The fiber diameter in the non-woven mats was found to be in the range of 150-500 nm. The silica that was amphiphilic in nature initially was converted into amphiphobic upon FAS modification. A water contact angle of 154° and 144° was obtained for water and oil, respectively (**Fig. 29**). Also a high heat resistance was exhibited by the fluorinated inorganic fibrous mats. Such a developed mat can be used for several potential applications such as high temperature filtration, selective filtration and self-cleaning coatings. Choi *et al*.[205] used electrospinning technique to fabricate fluoro-compound fibres, forming a web structure (**Fig. 30**) showing superamphiphobicity. Superamphiphobicity was exhibited by electrospun web of poly(2,2,2-trifluoroethyl methacrylate) fibres. The water contact angles for both water and hexadecane exceeded 150°. By varying the polymer solution concentration from 24 to 30 wt. %, modulation of web was achieved with other fixed processing conditions. The polymer concentration indeed affects the fibre diameter length. Smaller and uniform fiber diameter was observed when 26 wt. % solution was used to prepare the web. A simple method of dispersion polymerization of solution of methanol encompassing perfluoroalkyl methacrylates was employed by Yoshida[206] in preparing superamphiphobic surface that constituted of micro- and nanospheres. Microspheres were obtained by the polymerization of 2,2,2-trifluoroethyl methacrylate (TFMA) which had an average diameter of 4-12

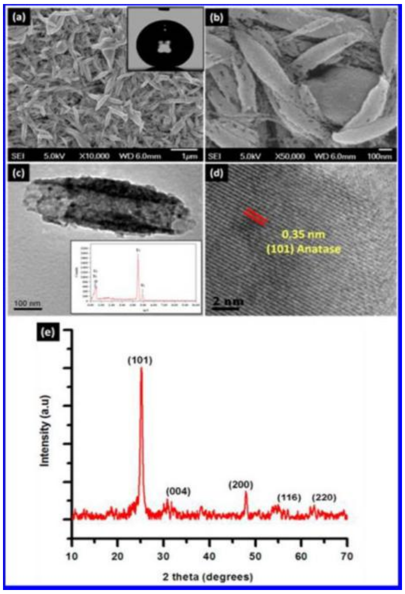

Fig. 26 (a,b) Higher and lower magnification of SEM image of TiO2 coated samples; **c)** TEM image of single nano-rice structure; **d)** resolved image of lattice e) XRD pattern of 500 °C sintered TiO_2 coated sample.[198]

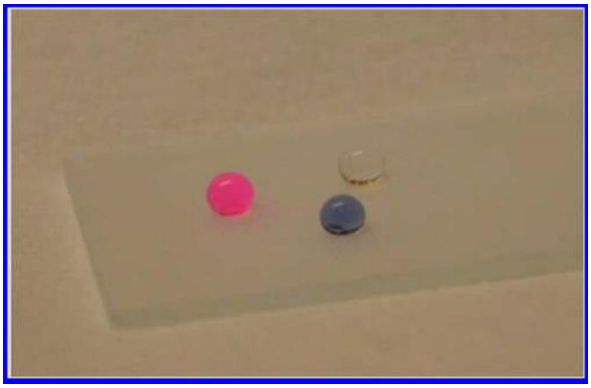

Fig. 27 Photograph depicting superamphiphobic surface with water(blue; dyed with trypan blue dye), glycerol(pink; dyed with rhodamine B) and ethylene glycol(colourless) droplets.[198]

μm. Nanospheres were obtained by the polymerization of 2-(perfluorooctyl)ethyl methacrylate (POMA) yielding an average diameter of 679 nm. Superamphiphobicity was shown by the surfaces coated with spheres. Water contact angles of 150° and 173° was obtained for PTFMA microspheres and PPOMA nanospheres, respectively, whereas a water contact angle of 159° and 160° was obtained for diiodomethane microspheres and diiodomethane nanospheres, respectively. The superamphiphobicity was produced due to the synergestic effects of spherical structure and high concentration of Fluorine, observed on the top surface (confirmed with X-ray photo electron spectroscopy analysis). A remarkable superamphiphobic coating (**Fig. 31**) was fabricated by Deng *et al.*[207a], which was oil-rebounding and transparent in nature. The candle soot was collected which was porous in nature. Onto them, thick silica shell of 25 nm was coated. Upon calcination at 600°C, the transparency was observed on the black coating. Superamphiphobic nature was attained after silanization. Sand impingement was done to test durability and it was observed that even though the top layer was damaged, the superamphiphobic nature was retained. Barthwal *et al.*[207b] employed anodization technique to fabricate superamphiphobic functional Ti foils. Maximization of contact angle of water and various oils were achieved using a two-step anodization method (**Fig. 32**) in which the voltage supply and anodization time were varied. Superamphiphobicity was controlled by the morphology of TiO_2 nanotube surface. Good superamphiphobic stability was observed for the anodized surface along with long-term storage. Also reversible switching of wetting property from hydrophobic and oleophobic to hydrophilic and oleophilic was observed for water and oil respectively and vice-versa via fluorination and air-plasma treatment. Such a developed technique could be used to fabricate amphiphobic Ti surfaces with large area 3-D surfaces. Mou *et al.*[208] fabricated amphiphobic epoxy coatings, deposited on silicon wafers. The coatings encompassed a mixture of bisphenol A diglycidyl ether, tetraethylorthosilicate (TEOS) and fluorinated side chain (F-silicon)- containing alkoxy silane. Water and oil Contact angle measurements were done to ensure the amphiphobic

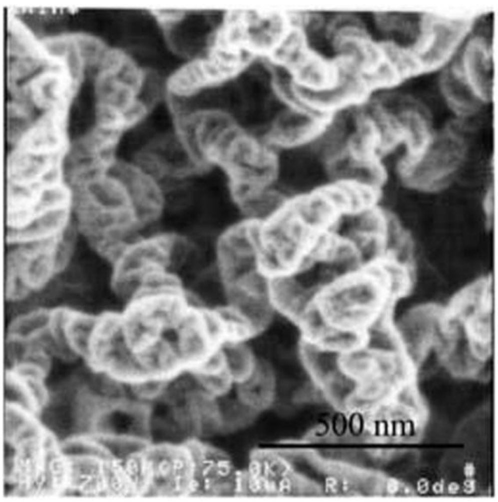

Fig. 28 SEM image of Ar-plasma treated (7 min) cross-linked benzoxazine film which has heated for 1 h at 200 °C and treated with CF_4 plasma (30s).[203]

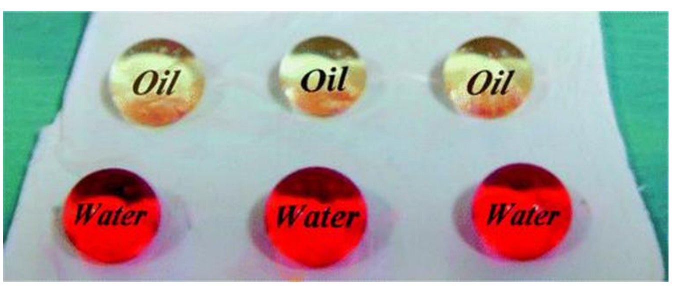

Fig. 29 Photograph showing the oil and water droplets on silane modified electrospun pure silica nanofibrous mat.[204]

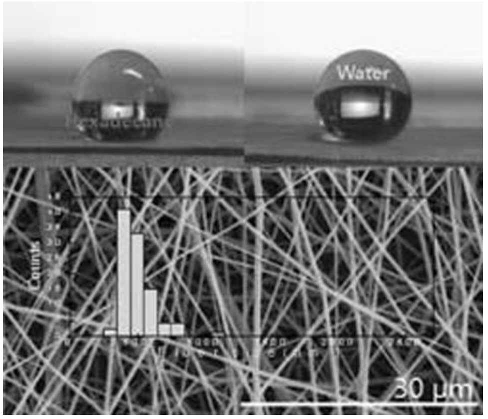

Fig. 30 SEM image of fluoro-compound fibers with a web structure(below), hexadecane (left) and water (right) droplets on the web surface showing its superamphiphobicity.[205]

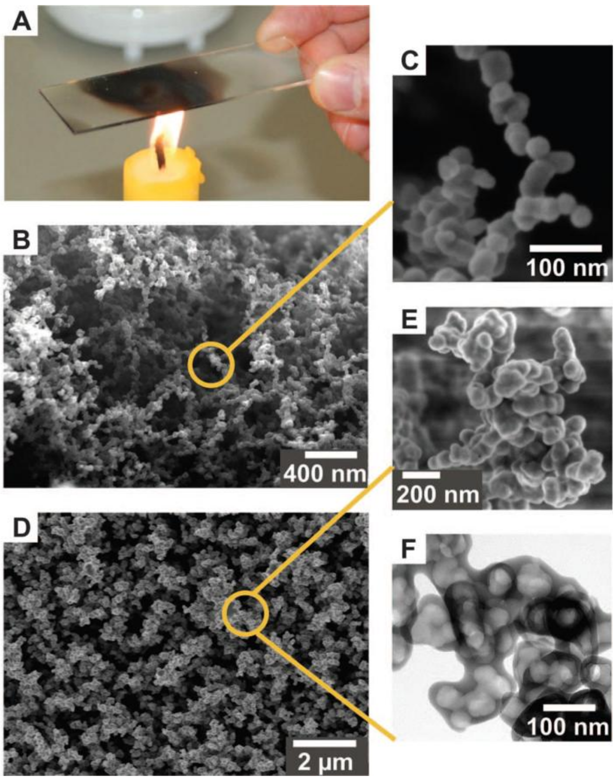

Fig. 31 (a) Figure indicating the candle soot preparation; (b) SEM image of the candle soot; (c) SEM image of the candle soot with high resolution; (d) SEM Image of the candle soot coated with silica shell; (e) and (f) SEM and TEM image of the calcined candle soot/silica shell mixture respectively.[207a]

behavior of the film. Ten nm thick epoxy ultrathin films were deposited on silicon wafer and to attain amphiphobicity, nominal fluorinated silane was added to the epoxy coatings. The sub-micrometer granules present in ultrathin coatings retained the surface lyophobicity. By adding tetraethylorthosilicate, the film hardness was improved. Ganesh *et al.*[209a] fabricated superamphiphobic coating using electrospun nanofibers that has one-dimensional morphology. The resultant coating was transparent and robust. By depositing a thick layer of SiO_2 nanofibers on glass, the template was created. An ultrathin porous silica membrane (25 nm) was deposited on the SiO_2 nanofiber template by vapour deposition process. A hybrid silica network (silica membrane enclosing SiO_2 nanofibers) (**Fig. 33**) was obtained upon heat treatment at 600 °C and the resultant coating was found to be transparent and superhydrophilic in nature. Reinforcement of SiO_2 nanofibers were done by the coated silica membrane during the heat treatment process and assist in preventing the disintegration of nanofibers into nanoparticles. A high roughness and surface texture was observed with such fiber morphology. The coating exhibited superamphiphobic property upon silanization. The contact angle measurements showed a value of 161° and 146.5° for water and hexadecane respectively. With aluminium (Al) plate as substrate, Barthwal *et al.*[209b] fabricated a superamphiphobic surface **(Fig. 34)** on the surface which was mechanically robust. By using a combination of chemical etching and anodization technique, micro and nanoscale structures were developed on Al plate surface. This surface showed super-repellent behaviour towards liquids (evident from wettability measurements) whose surface energy falls in the range of 27.5-72 mN/m. The effects of morphological change on wettability was analysed by changing the anodization time. Scotch tape and hardness tests revealed that the prepared surface had good adhesion and mechanical durability, respectively.

By combining fluorinated poly urethane (FPU) containing a terminal perfluoroalkane segment and incorporated SiO_2 nanoparticles, Wang et al.[209c] fabricated nanofibrous membranes encompassing superamphiphobic nature which exhibited breathable and robust water/oil proof performances. A water contact angle of 165° and oil contact angle of 151° were observed for FPU/SiO_2 nanoparticles incorporated hybrid membranes revealing superhydrophobic and superoleophobic characteristics, respectively. By tuning the surface composition as well as hierarchical structures, wettability of resultant membranes could be manipulated which was confirmed using surface morphological studies.

8. Multifunctional Coatings

Multifunctional coatings, as the name suggests have a wide range of potential applications with greater degree of control and scalability. Multiple properties can be encompassed into such coatings such as scratch-resistance, self-cleaning property, anti-icing, self-healing, anti-reflective property etc. Haeshin *et al.*[210] used a simple dip-coating technique to fabricate multifunctional polymer coatings in an aqueous solution of dopamine. To biomimic the adhesive proteins in mussels, a thin film of polydopamine was developed using dopamine self-polymerization. These films were used for a range of substrates like polymers, ceramics, noble metals, oxides etc. Additional layer could be deposited using secondary reactions such as electrode-less metallization for depositing metal films, macromolecule grafting for bio-inert and bioactive surfaces etc. Wei *et al.*[211] used oxidant-induced polymerization to synthesize polydopamine coatings which can be prepared in acidic/neutral/alkaline aqueous media. Such coatings are found to be multifunctional as well as material-independent. Inspired by the moth eyes which are antireflective and the cicada wings which are superhydrophobic in nature, Sun *et al.*[212] tried to biomimic both these functionalities by fabricating multifunctional optical coatings (a template technique). Using soft-lithography process, fluoropolymer nipple arrays are created which are subwavelength-structured. The enhancement of both anti-reflective and hydrophobic functionalities is done by the utilization of fluoropolymers. An experiment and modelling have been done to study the effect of size and crystalline ordering of the replicated nipples on the antireflective property. Such coatings find extensive applications in antireflection self-cleaning coatings. Dingremont *et al.*[213] tried to combine both physical vapor deposition and nitriding treatment in synthesizing multifunctional coatings which made the coating to withstand higher loads, thus improving their mechanical strength. The thermal stability of the iron nitride layers was affected by the coating conditions. To synthesize biomedical coatings, layer-by-layer assembly finds a great deal, which is also shown for local drug delivery systems. But such hydrophobic drugs have a drawback of poor loading capacity. Hu *et al.*[214] tried to provide nanoreservoirs for such hydrophobic molecules (guest) by the incorporation of sulphonated hyperbranched polyether (HBPO-SO_3) with a hydrophobic core onto Layer-by-Layer (LbL) films. For LbL assembly into a buffer solution of sodium acetate and acetic acid, HBPO-SO_3 formed stable micelles. Quartz crystal microbalance (QCM) measurements and

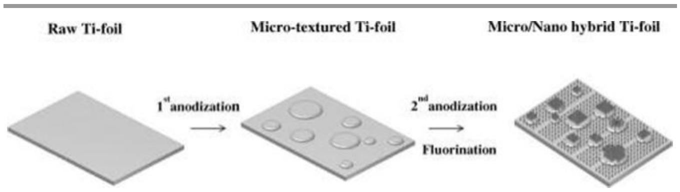

Fig. 32 Figure showing the two-step anodization method of preparation of superamphiphobic functional Ti foils.[207b]

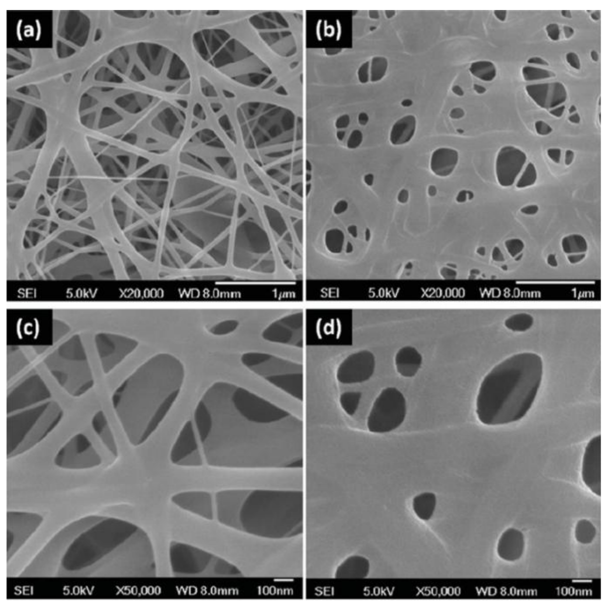

Fig. 33 (a) and **(c)** low and high magnification SEM images of SiO_2 nanofibers as-spun. **(b)** & **(d)** - low and high magnification SEM images of Silica which forms a hybrid network (silica membrane enclosing SiO_2 nanofibers).[209]

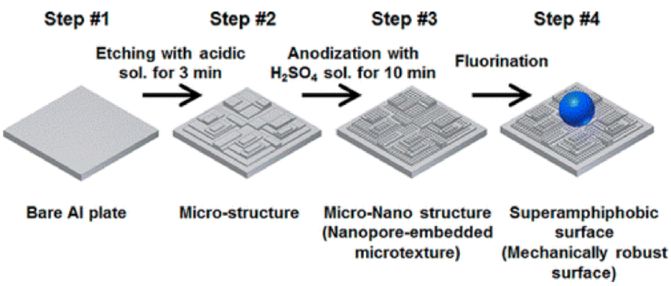

Fig. 34 Schematic diagram showing the various steps for fabricating superamphiphobic surface on Aluminium substrate.[209b]

ellipsometry experiments exemplified that HBPO-SO_3 micelles and chitosan can be deposited in an alternating fashion so as to form LbL films. Controlled release of guest molecules into LbL films was achieved using post-diffusion process (incorporation of hydrophobic pyrene). Using post-diffusion of anti-restenosis agents into HBPO-SO/chitosan multilayer film, a multifunctional coating was fabricated that prevents restenosis after coronary angioplasty. Such a coating was found to possess anticoagulation, anti-bacterial and local release of hydrophobic drug Probucal (powerful antioxidant property). Cebeci *et al.*[215] used LbL assembly method to fabricate multifunctional nanoporous thin films from silica nanoparticles and a polycation. Both anti-reflection and anti-fogging properties were shown by the synthesized multifunctional coating. Superhydrophilic wetting characteristics were developed in the coating which caused the anti-fogging property. The WCA was found to be < 5°. The light scattering water droplets was prevented from forming on a surface by using such characteristic superhydrophilic wetting surface. The presence of nanopores yielded low refractive index for the film (1.22) which in turn imparted good antireflective properties. Transmission of 99.8% was recorded for the multilayer films coated on both sides of a glass slide. The stability of superhydrophilic wetting characteristics was considered by a critical number of bilayers which was deposited on surface. The film property is also affected by the choice of nanoparticle size, nanoparticle concentration, pH of the solution etc. Yuan *et al.*[216] used LbL assembly technique to fabricate a multilayered multifunctional coating encompassing TiO_2 and Ag nanoparticles and the TiO_2 nanoparticles served as contact-active antibacterial agent whereas the nanosilver acted as active antibacterial agent. Crystalline anatase TiO_2 nanoparticles were synthesized by sol-gel method and the assemblage of TiO_2 nanoparticle-chitosan with heparin through LbL assembly was substantiated with the results obtained from AFM, QCM and Contact angle measurements. The loading silver nanoparticles onto the multilayers and was proven using UV-visible spectroscopy. The bactericidal effect of nanosilver loaded TiO_2 – chitosan/heparin multilayers was confirmed with a short-term antibacterial assay, which was done in dark and low-intensity UV. Voevodin *et al.*[217] investigated self-assembled nanophase particle (SNAP)-based nanostructured surface treatment coatings which can replace the chromate-based surface treatments on aluminium alloys used in aircraft industry. Such a process could be carried out in a low-temperature regime. This technique of designing coating components from the molecular level gives a key path in the fabrication of multi-functional coatings. To study the corrosion protection of aluminium alloys, organic inhibitors were used with SNAP. Jin *et al.*[218] used TiO_2 coating to fabricate a VO_2 thermochromic film for window structure. Compared to SiO_2, TiO_2 showed excellent anti-reflective properties. Such a coating becomes multifunctional with an effect of excellent photocatalytic properties. An increment in luminous transmittance by 53% was observed for these coatings. The window structure synthesized has the capability of UV stopping, automatic solar/heat control with luminous transmission and photocatalytic functions, thus rendering it multifunctional. Zhao *et al.*[219] presented a review on multifunctional coatings based on TiO_2 multilayer film and other functional coatings, which are applied as photoactive material in the glasses. Using sol-gel method, TiO_2 photocatalyst-based thin films (nanoporous) can be synthesized which is superhydrophilic in nature and shows self-cleaning effect. By treating the films in acidic solutions, the photocatalytic activity of soda-lime glass coated with TiO_2 thin films can be enhanced. Excellent photo-induced antibacterial property was also shown by the film. Silver in small amounts is added to TiO_2 porous film so as to enhance its anti-bacterial effect in the absence of UV radiation. To make the TiO_2 thin films functionalize as self-cleaning glass in visible region, appropriate heat treatments are done. To yield low-E self-cleaning glasses, a multilayer of $TiO_2/TiN/TiO_2$ was deposited on the glass substrate. Lauridsen *et al.*[220] used direct current magnetron sputtering of Ti_3SiC_2 compound target at a deposition rate of 16 μm/h to deposit Ti-Si-C coatings (amorphous and nanocomposite) onto high speed steel, SiO_2 and Si substrates. The deposition was carried out at a temperature of 200 or 270 °C. By changing the pressure to 4 mTorr and target to substrate distance to 2 cm, nanocrystalline coating can be modified into amorphous type. To impart superhydrophobicity, self-cleaning and UV blocking properties, Ates *et al.*[221] synthesized cotton fabric loaded with zinc oxide nanowires. Microwave-assisted hydrothermal method was used to grow ZnO nanowires and a WCA of 150° was observed upon functionalizing with stearic acid exemplifying its

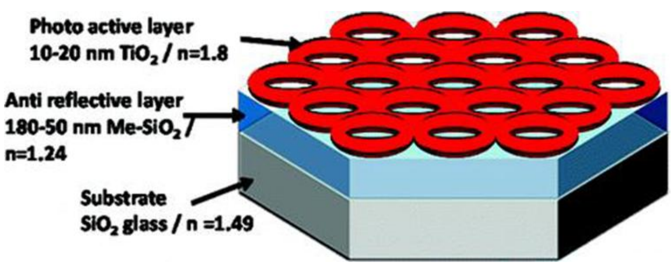

Fig. 35 Schematic representation of multifunctional SiO_2/TiO_2 bilayer on glass substrate.[225]

superhydrophobic nature. A decrement in UV transmission was observed for the synthesized cotton fabric. Degradation of methylene blue under UV irradiation exhibited self-cleaning activity of cotton fabric coated with ZnO nanowire. The synthesis of inorganic-organic transparent multifunctional coatings can be done by the sol-gel synthesis of ceramic colloidal particles in which particle size is maintained in lower nano-range. The synthesis is carried out in the presence of organo-alkoxy silanes. With this approach, Schmidt[222] fabricated a multifunctional coating with anti-fogging, anti-soiling properties with low-surface energy and thermal stability upto 350 °C. Spinning technique involving incorporation of ZnO nanoparticle into inorganic/organic hybrid matrices was carried out by Li *et al.*[223] in order to fabricate multifunctional inorganic/organic nanocomposite coatings on poly(methyl methacrylate)(PMMA). From tetraethoxysilane (TEOS) and 3-glycidyloxypropyl trimethoxycilane (GLYMO), hybrid matrices were derived. The interface between nanoparticles and organic groups was modified so as to protect the polymer structure from destruction, caused by ZnO. The coatings thus obtained are UV absorbent, dense, flexible and abrasion resistant. Dervishi *et al.*[224] investigated a novel method to control bulk and surface electrical conductivity of polymeric films. The electrical bulk resistivity was decreased by several orders of magnitude upon addition of Carbon Nanotubes (CNTs) in small amounts into the polymeric material. Also the polymeric surface films were electrosprayed with nanolayers of single and multiwall CNTs and surface resistivity was analyzed as a function of nanotube loading. High charge dissipation rates were observed for CNT modified surfaces. Faustini *et al.*[225] used sol-gel technique to deposit a multifunctional coating with photocatalytic, hydrophobic, anti-fogging and anti-reflective properties. Sol-gel liquid deposition of two successive oxide layers (**Fig. 35**) was done to fabricate such multifunctional coatings. Nanoporous SiO_2 material with high mechanical stability, transparency and water resistance functionalized with methyl groups constituted the first layer. The anti-reflective property could be controlled by selecting proper processing and chemical conditions so as to control thickness and refractive index. On the top of this anti-reflective layer, ultrathin TiO_2 layer was deposited which was crystalline and nanoperforated. This layer ensures antifogging, photocatalysis and exhibit a barrier towards mechanical aggressions. Organic species adsorbed into anti-reflective layer was photo-decomposed. The coatings have high mechanical and chemical durability and can be produced at low cost. Such multifunctional coatings are great potential candidates for Photovoltaic cells. A combined sol-gel, dip-coating process was carried out by Miao *et al.*[226] in fabricating multifunctional coatings of double-layered SiO_2-TiO_2 coatings on glass substrates wherein the successive oxide layer deposition was done. The multifunctional coating encompassed both anti-reflective and self-cleaning property. Hybrid methyl –functionalized nanoporous SiO_2 material forms the first layer with an anti-reflection gain of 6%. By adjusting the thickness and by selecting suitable solvents and pore-forming agents, thickness and refractive index of the coating could be controlled. An ultrathin layer which is nanoporous in nature forms the second layer. This layer has dual

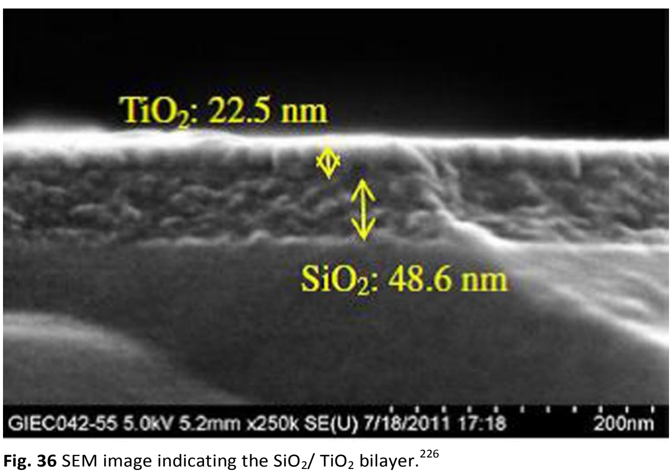

Fig. 36 SEM image indicating the SiO_2/ TiO_2 bilayer.[226]

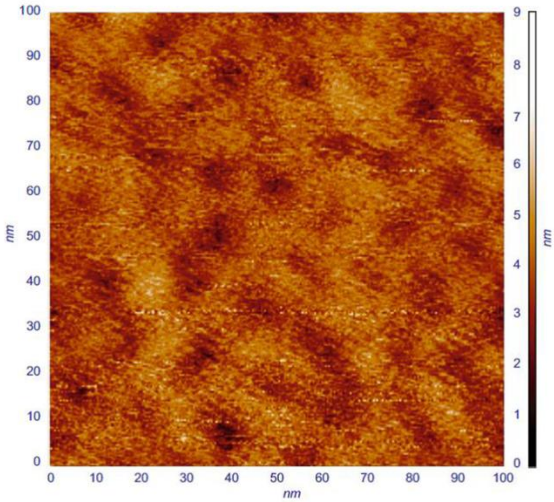

Fig. 37 AFM image (top view) of TiO_2 mesoporous layer.[227]

functionalities: ensures self-cleaning and prevents mechanical damage. By SiO_2/TiO_2 bilayers (**Fig. 36**), 3.4% anti-reflectivity is obtained (400-800 nm). The band-edge absorption in TiO_2 can be compensated by controlling the pore-size distribution in SiO_2 layer. The coating synthesized has high mechanical and chemical durability and can be used for solar cells as large substrates. The coatings that provide high transmittance along with self-cleaning capacity are the herald for glasses and glazing materials for solar applications. Prado *et al.*[227] fabricated a multifunctional coating comprising both self-cleaning and anti-reflective property. By controlling the solvent and template agent ratio, film thickness and nanostructure could be controlled thereby monitoring transmittance and refractive index of each layer. The multifunctional coating had a stack layer of SiO_2 (anti-reflective) and dense TiO_2 (mesoporous) (**Fig. 37**) layer. A higher degree of photodegradation of organic matter was achieved for mesoporous TiO_2 layers compared to dense TiO_2 layer. A net transmission of 95.9% and 96.6% was achieved for multifunctional and anti-reflective coatings. Son *et al.*[228] demonstrated that a superhydrophilic glass without surface chemical treatment showed high anti-reflective and self-cleaning effects. As a result, an outdoor test for 12 weeks (**Fig. 38**) showed only 1.39% of solar efficiency drop compared to 7.79% and 2.62% efficiency drop for bare glass and superhydrophobic packing. Due to the reflection of incident light at air/glass interface and through the scattering effect (due to dust accumulation), the incident energy is lost on solar modules. Even though certain anti-reflective coatings can remedy dust accumulation, still this problem remains critical that affects the efficiency. Verma *et al.*[229] reported a reduction of reflection at air/glass interface and enhanced self-cleaning property by non-lithographic nanostructuring of packaging glass surface (**Fig. 39**). Upon nanostructuring, superhydrophilic property is shown by the glass surface with a CA < 5°, thus proving to be a better self-cleaning coating. Liu *et al.*[230a] fabricated a multifunctional coating of SiO_2/TiO_2 bilayer *via.* sol-gel dip-coating method with self-cleaning and anti-reflective properties. Due to the lower refractive index, SiO_2 layer (bottom) acts as anti-reflective coating whereas TiO_2 layer (top) models self-cleaning coating (combination of photocatalysis and photo-induced superhydrophilicity). Irrespective of high refractive index and coverage of TiO_2 nanoparticles, a transmission of 96.7% was achieved by

SiO_2/TiO_2 bilayer. However, the effect of coverage due to TiO_2 nanoparticles had a control over the photocatalytic property of the bilayer synthesized. Great self-cleaning functionality was observed when UV light was irradiated on SiO_2/TiO_2 bilayer film and the water contact angle was found to be less than 2°.

Tang et al.[230b] fabricated a novel nanofibrous membrane modified with fluorinated polybenzoxazine (F-PBZ) to achieve gravity driven oil-water separation. By combining electrospun poly (m-phenylene isophthalamide) (PMIA) nanofibers and SiO_2 nanoparticles-incorporated polymerized (in situ) F-PBZ functional layer, realization of membrane design was achieved. The pristine hydrophilic PMIA nanofibrous membranes upon modidication with F-PBZ/SiO_2 nanoparticle showed a water contact angle of 161° and oil contact angle of 0° revealing superhydrophobicity and superoleophilicity, respectively. Such a membrane showed excellent thermal and mechanical stability and good hot water repellency. Also the as-prepared membranes prove to be a good candidate for industrial oil-polluted water treatments and oil spill clean-up due to their fast and efficient oil-water separation by a solely process driven by gravity.

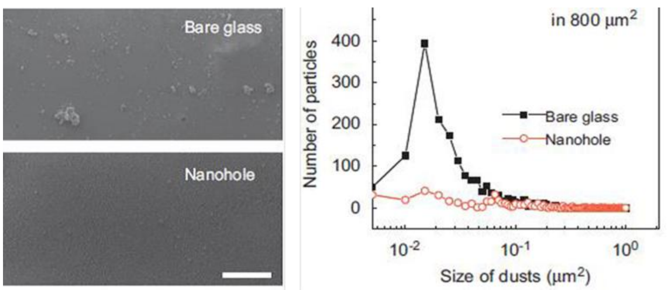

Fig. 38 Left side shows the SEM image of bare glass(top) and Nanohole (bottom) which have undergone a 12 week outdoor test. The right side shows the graph depicting the strength of self-cleaning effect for Nanohole which has lesser number of particle on 800 μ m^2 (dust) even after 12 week outdoor test.[228]

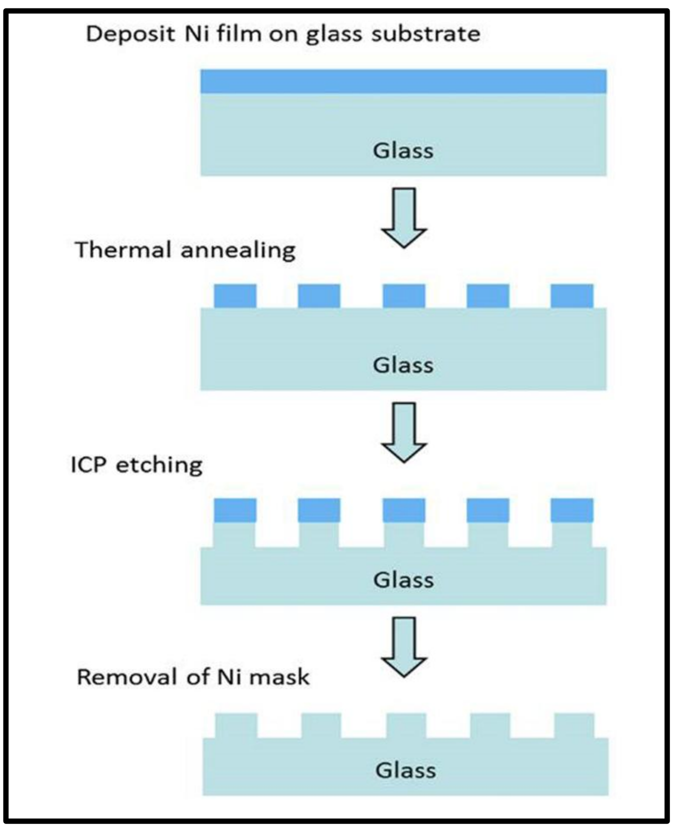

Fig. 39 Schematic diagram elucidating steps involved in non-lithographic nanostructuring of packaging glass surface.[229]

New synthesis methods have been developed inorder to combine both oleophobic and hydrophilic character in coatings so as to overcome the limitation of thermodynamic surface energetics. Such smart surfaces possess different functional groups with favourable and unfavourable interaction with polar and non-polar liquids, respectively.[231a] In such smart surfaces, intercalation of oleophobic and hydrophilic constituents occur. Oleophobic character is obtained when the interface, in presence of oil droplets gets occupied by low-surface energy component. Nevertheless, due to the hydrophilic components, water molecules penetrate through such surfaces. Recently spray casting technique of nanoparticle-polymer suspensions on various substrates was used to fabricate nanocomposite coatings that encompass both superhydrophilicity and superoleophobicity.[231b] Such a dual character is due to the combined cooperation of oleophobic-hydrophilic groups of PFO-PDDA and hierarchical surface structures. Fluorinated groups in high surface concentration occupied the interface in the presence of oil indicating superoleophobic nature of the surfaces. Due to the surface molecular re-arrangement induced by water, water molecules could penetrate through these surfaces. Coatings with such dual character find immense practical application in oil/water separation. By the reaction between fluoroalkanoyl peroxides with trimethoxyvinylsilane and acryloylmorpholine, resulted in fluoroalkylated flip-flop silane coupling agents that contains morpholino groups. Such silane coupling agents are used to modify glass surfaces which exhibited both hydrophilic and oleophobic character.[232a] Similarly fluorinated sulfonic acid co-oligomer/SiO_2 polymer hybrid was used to modify glass surfaces which exhibited both oleophobicity and hydrophilicity.[232b] Using covalently grafted f-PEG, surfaces with oleophobic-hydrophilic nature was constructed by a grafting approach. Solvent-sensitive stimuli-responsive properties were exhibited by the f-PEG polymer brush coatings which also showed hydrophilic-oleophobic behaviour. Oleophobic-hydrophilic polymers with stimuli responses are a great venture for the fabrication of next generation anti-fogging and self-cleaning coatings.[232c,d]

The frequent oil-spill accidents and increasing industrial oily wastewater (which destroys the aquatic species) demand worldwide challenge in oil/water separation. Conventionally special wetting materials with simultaneous superhydrophobicity and superoleophilicity were used for oil/water separation.[233a-c] Recently, a novel mesh coated with PAM hydrogel which exhibited superoleophobicity underwater and superhydrophilicity in air was fabricated to tackle the oil/water separation.[234a] Without any extra power, water from oil-water mixtures such as vegetable oil, diesel etc. was removed effectively and selectively by the obtained mesh **(Fig. 40**). Such meshes coated with hydrogel possess promising advantages compared to traditional hydrophobic and oleophobic materials such as high efficiency, resistance to oil fouling and easy recyclability. Introduction of smart materials like stimuli-responsive polymers on porous materials is a new attempt for oil/water separation. A smart surface has been fabricated on porous textiles or polyurethane sponges using block copolymer comprising oleophilic/hydrophobic PDMS and pH-responsive P2VP blocks.[234b] Such porous materials in aqueous media have a switchable superoleophobic-superoleophilic characteristic which can be used for effective water/oil separation. A photo-responsive surface with aligned ZnO nanorod array was used for water-oil separation.[234c] Switchable superhydrophobicity-superhydrophilicity and underwater superoleophobicity was possessed by stainless steel

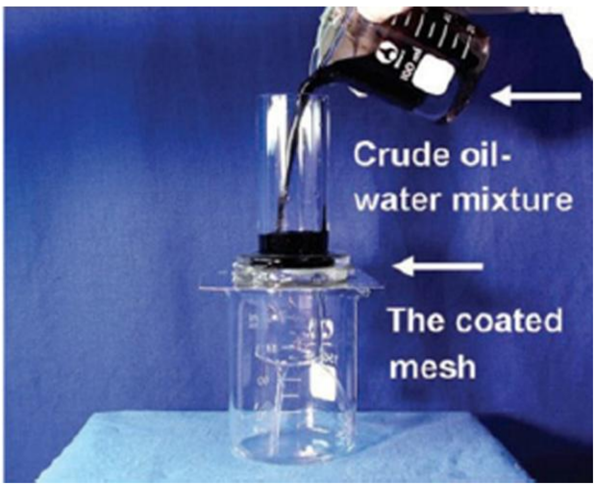

Fig. 40 Image showing the oil/water separation process in which a coated mesh is used for the separation purpose.[230l]

mesh films coated with ZnO which exhibited highly controlled separation efficiency of oil/water mixtures.

Inspired from self-cleaning lotus effect, Zhang et al.[235] has fabricated a polyurethane foam which encompasses both superhydrophobicity and superhydrophilicity. The as-prepared foam floats easily on water due to its low-density, light weight and superhydrophobicity (**Fig. 41**). Multifunctional properties are demonstrated by the foam like material in oil/water separation, super-repellency towards corrosive liquids and self-cleaning. Such low-cost process is promising for the design of multifunctional foams that can be used for oil-spill clean-up in larger areas.

By combining electrospun cellulose acetate (CA) nanofibers and silica nanoparticles-incorporated polymerized fluorinated poly benzoxazine (F-PBZ) functional layer, Shang et al.[236] fabricated nanofibrous membranes encompassing superhydrophobic and superoleophilic character which exhibited robust oil-water separation. A water contact angle of 161° and oil contact angle of 3° was observed by employing F-PBZ/SiO_2 nanoparticles modification revealing superhydrophobicity and Superoleophobicity, respectively. The as-prepared membranes are a promising candidate in industrial oil-polluted water treatments and oil spill clean-up as they exhibited excellent stability over a wide range of pH conditions and efficient separation of oil-water mixtures.

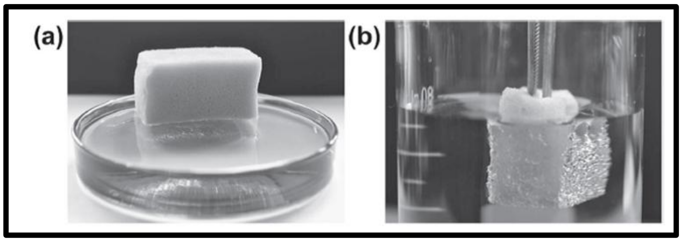

Fig. X2 a) The optical image of the water floating as-prepared polyurethane foam which reveals its light weight and superhydrophobicity, b) Digital image showing the Superhydrophobic foam which is immersed in water by an external force and as such the air bubbles surround the foam exhibiting a silver mirror-like surface.[230o]

Due to unique pore character, excellent chemical, thermal and mechanical stability, zeolite films have attracted intense research for oil-water separation. Wen et al.[237] demonstrated oil-water separation driven by gravity using mesh films coated with zeolite. The zeolite surface possessed excellent superhydrophilicity and underwater superoleophobicity that finds high efficiency separation of various oils. By tuning the pore size, the flux and intrusion pressure could be tuned. Also such films are promising candidates in oil-water separation because of their corrosion-resistant character in the presence of corrosive media.

Zhang et al. [238] fabricated PAA/PDDA silicate multilayer films by alternatively depositing complexes of poly (diallyldimethyl ammonium chloride) (PDDA) and sodium silicate (PDDA-silicate) with poly (acrylic acid), (PAA). Highly porous silica coatings with excellent substrate adhesion and mechanical stability were produced by calcinating PAA/PDDA-silicate multilayer films in which the organic components were removed. Such porous silica coatings covering quartz substrates exhibit antireflection and antifogging properties as the resultant films possess reduced refractive index and superhydrophilic nature. High porosity could be introduced to the resultant silica coatings by the use of PDDA-silicate complexes which favors the fabrication of coatings encompassing antireflection and antifogging properties with enhanced performance. Rapid fabrication of porous silica coatings is facilitated by PDDA-silicate complexes after calcination due to the larger dimensions of solution complexes.

Conclusions

Smart self-cleaning coatings are those which respond to external influences such as electric field, temperature, light, etc. Researchers are inspired by the nature's boundless kaleidoscopic effects and they try to biomimic them to create artificial structures almost close to the nature's phenomenon. Self-cleaning basically comprising hydrophobic and hydrophilic coatings has been reviewed. It is already being reflected in our daily life like the silver nano-coated clothes, water proof- paints, shoes, umbrellas, etc. In TiO_2-based photocatalytic-hydrophilic coatings, further research should focus on broadening the absorption wavelength range of the photocatalysts since the photocatalytic effect of the TiO_2 coatings is UV light-based which just represents ~ 4% of the solar spectrum and hence the efficiency of the photocatalytic effect is minimum. Other potential coatings that possess various real applications such as oleophobic coatings, amphiphobic coatings and multifunctional coatings have also been reviewed. The multifunctional coating is an open area where further research can be motivated. It will find immense applications in glass industry, medical field (drug-targeting, self-healing), solar cells, etc. New synthesis and surface modification routes need to be developed which can provide excellent adhesion and strength for the coating on the substrates used. Other areas of investigation will probably be the study of toxicity of such coatings, so that it can be applied safely in real applications like water purification membranes, self-repair-, self-healing- and self-lubricating coatings, etc. Even though large research focus is going in for fabrication of such coatings, these synthesis routes need to be developed which are cost-effective but without compromising the quality.

Acknowledgements

The authors thank the Ministry of New and Renewable energy (MNRE), Government of INDIA for financial support.

[a] Amrita Centre for Nanosciences and Molecular Medicine, Amrita Institute of Medical Sciences, Amrita Vishwa Vidyapeetham University, AIMS Ponekkara PO, Kochi 682041, Kerala, India. Email: sreekumarannair@aims.amrita.edu
[b] Engineering Product Development (EPD) Pillar, Singapore University of Technology and Design (SUTD), 20 Dover Drive, Singapore - 138682.

References

1 (a) V. A. Ganesh, H. K. Raut, A. S. Nair and S. Ramakrishna, *J. Mater. Chem.*, 2011, **21**, 16304-16322. (b) M. Yasuhiro, D. Bin and S. Seimei, *Nanotechnology*, 2006, **17**, 5151.
2 W. Barthlott and C. Neinhaus, *Planta.*, 1997, **202(1)**, 1-8.
3 X. Gao and L. Jiang, *Nature*, 2004, **432(7013)**, 36.
4 G. Zhang, J. Zhang, G. Xie, Z. Liu and H. Shao, *Small*, 2006, **2(12)**, 1440-1443.
5 H. Lee, B. P. Lee and P. B. Messersmith, *Nature*, 2007, **448(7151)**, 338-341.
6 D. Byun, J. Hong, Saputra, J. H. Ko, Y. J. Lee, H. C. Park, B-K. Byun and J. R. Luker, *J.Bionic Eng.*, 2009, **6(1)**, 63-70.
7 I. P. Parkin and R. G. Palgrave, *J. Mater. Chem.*, 2005, **15**, 1689-1695.
8 *http://www.lotusan.de/ (in German)*
9 *http://www.activglass.com/index_eng.htm*
10 *http://www.ppg.com/.*
11 K. Hashimoto, H. Irie and A. Fujishima, *Jpn. J. Appl. Phys.*, 2005, **44** 8269-8285.
12 X. Feng, L. Feng, M. Jin, J. Zhai, L. Jiang, and D. Zhu, *J. Am. Chem. Soc.*, 2004, **126**, 62-63.
13 A. Lafuma and D. Quéré, *Nat. Mater.*, 2003, **2**, 457-460.
14 N. Nuraje, Waseem S. Khan, Y. Lei, M. Ceylan and R. Asmatulu, *J. Mater. Chem. A*, 2013, **1**, 1929-1946.
15 J. Bico, C. Marzolin and D. Quere, *Europhys.Lett.*, 1999, **47**, 220-226.
16 D. Richard and D. Quere, *Europhys.Lett.*, 1999, **48**, 286-291.
17 D. Richard and D. Quere, *Europhys.Lett.*, 2000, **50**, 769-775.
18 P. Aussillous and D. Quere, *Nature*, 2001, **411**, 924-927.
19 D. Richard, C. Clanet and D. Quere, *Nature*, 2002, **417(6891)**, 811.
20 J. Bico, C. Tordeux and D. Quere, *Europhys. Lett.*, 2001, **55**, 214-220.
21 Ralf Blossey, *Nat. Mater.*, 2003, **2**, 301-306.
22 M. Miwa, A. Fujishima, K. Hashimoto, T. Watanabe, *Langmuir*, 2000, **16**, 5754-5760.
23 I. Sas, R. E. Gorga, J. A. Joines and K. A. Thoney, *J. Polym. Sci., Part B: Polym. Phys.*, 2012, **50**, 824-845.
24 A. B. D. Cassie, S. Baxter, *Trans. Faraday Soc.*, 1944, **40**, 546-551.
25 T. N. Wenzel, *J. Phys. Colloid Chem.*, 1949, **53**, 1455.
26 A. Nakajima, K. Hashimoto and T. Watanabe, *Monatsch. Chem.*, 2001, **132**, 31-41.
27 R. Blossey, *Nat. Mater.*, 2003, **2**, 301-306.
28 Q. Zhu, Q. Gao , Y. Guo , C. Q. Yang , and L. Shen, *Ind. Eng. Chem. Res.*, 2011, **50 (10)**, 5881-5888**.**
29 Z. Guo, W. Liu and B. L. Su, *J. Colloid Interface Sci.*, 2011, **353(2)**, 335-355.
30 L. Cao, T. P. Price, M. Weiss and D. Gao, *Langmuir*, 2008, **24**, 1640-1643.
31 A. Vilcnik, I. Jerman, A. Surca Vuk, M. Kozelj, B. Orel, B. Tomsic, B. Simoncic and J. Kovac, *Langmuir*, 2009, **25**, 5869-5880.
32 S. S. Chhatre, A. Tuteja, W. Choi, A. Revaux, D. Smith, J. M. Mabry, G. H. McKinley and R. E. Cohen, *Langmuir*, 2009, **25(23)**, 13625-13632.
33 W. Choi, A. Tuteja, S. Chhatre, J. M. Mabry, R. E. Cohen and G. H. McKinley, *Adv.Mater.*, 2009, **21** , 2190-2195.
34 R. Misra, R. D. Cook and S. E. Morgan, *J. Appl. Polym. Sci.*, 2010, **115**, 2322-2331.
35 P. Muthiah, S. H. Hsu and W. Sigmund, *Langmuir*, 2010, **26**, 12483 - 12487.
36 Y. Y. Yan, N. Gao and W. Barthlott, *Adv. Colloid Interface Sci.*, 2011, **169**, 80 - 105.
37 R. N. Wenzel, *Ind. Eng. Chem.*, 1936, **28**, 988-994.
38 M. Miwa, A. Nakajima, A. Fujishima, K. Hashimoto and T. Watanabe, *Langmuir*, 2000, **16**, 5754-5760.
39 R. E. Johnson and R. H. Dettre, *Adv. Chem. Ser.*, 1964, **43**, 112-135.
40 T. Onda, S. Shibuichi, N. Satoh and K. Tsujii, *Langmuir*, 1996, **12 (9)**, 2125-2127.
41 S. Shibuichi, T. Onda, N. Satoh and K. Tsujii , *J. Phys. Chem.*, 1996, **100 (50)**, 19512-19517.
42 C. Neinhuis and W. Barthlott, *Annu Bot.*, 1997, **79 (6)**, 667-677.
43 J. Bico, C. Marzolin and D. Quéré, *Europhys. Lett.*, 1999, **47**, 220.
44 S. Herminghaus, *Europhys. Lett.*, 2000, **52 (2)**, 165-170.
45 D. Oner and T. J. McCarthy, *Langmuir*, 2000, **16(20)**, 7777-7782.
46 Zen Yoshimitsu, Akira Nakajima, Toshiya Watanabe, and Kazuhito Hashimoto, *Langmuir*, 2002, **18 (15)**, 5818-5822.
47 X. Du, X. Li, J. He, *ACS Appl. Mater. Interfaces*, 2010, **2**, 2365-2372.
48 X. Li, X. Du, J. He, *Langmuir*, 2010, **26**, 13528-13534.
49 X. Du, J. He, *ACS Appl.Mater.Interfaces.*, 2011, **3**, 1269-1276.
50 P. C. Lin, S. Yang, *Soft Matter*, 2009, **5**, 1011-1018.
51 W. Ming , D. Wu , R. Van Benthem and G. de With, *Nano Lett.*, 2005, **5 (11)**, 2298-2301.

52 Z. Qian, Z. Zhang, L. Song, H. Liu, *J. Mater. Chem.*, 2009, **19**, 1297-1304.
53 B. Leng , Z. Shao , G. de With and W. Ming, *Langmuir*, 2009, **25 (4)**, 2456-2460.
54 X. Li, T. He, M. C. Calama, and D. N. Reinhoudt, *Langmuir*, 2008, **24 (15)**, 8008-8012.
55 W. Stober, A. Fink and E. Bohn, *J. Colloid Interface Sci.*, 1968, **26**, 62-69.
56 S. R. Coulson, I. Woodward, J. P. S. Badayal, S. A. Brewer and C. Willis, *J. Phys. Chem. B*, 2000, **104**, 8836-8840.
57 L. Feng, S. Li, Y. Li, H. Li, L. Zhang, J. Zhai, Y. Song, B. Liu, L. Jiang and D. Zhu, *Adv. Mater.*, 2002, **14**, 1857-1860.
58 C. Dorrer and J. Ruhe, *Soft Matter*, 2009, **5**, 51-61.
59 M.T. Khorasani, H. Mirzadeh and Z. Kermani, *Appl. Surf. Sci.*, 2005, **242**, 339-345.
60 M. Jin, X. Feng, J. Xi, J. Zhai, K. Cho, L. Feng and L. Jiang, *Macromol. Rapid Commun.*, 2005, **26**, 1805-1809.
61 M. Ma, R. M. Hill, J. L. Lowery, S. V. Fridrikh and G. C. Rutledge, *Langmuir*, 2005, **21**, 5549-5554.
62 J. Zhang, J. Li and Y. Han, *Macromol. Rapid Commun.*, 2004, **25**, 1105-1108.
63 J. Shiu, C. W. Kuo and P. Chen, *Chem. Mat.*, 2004, **16**, 561-564.
64 X. Lu, C. Zhang and Y. Han, *Macromol. Rapid Commun.*, 2004, **25**, 1606-1610.
65 R. Mohammadi, J. Wassink and A. Amirfazli, *Langmuir*, 2004, **20**, 9657-9662.
66 N. Zhao, J. Xu, Q. Xie, L. Weng, X. Guo, X. Zhang and L. Shi, *Macromol. Rapid Commun.*, 2005, **26**, 1075-1080.
67 J. Zhang, X. Lu, W. Huang and Y. Han, *Macromol. Rapid Commun.*, 2005, **26**, 477-480.
68 X. Feng, L. Feng, M. Jin, J. Zhai, L. Jiang and D. Zhu, *J. Am. Chem. Soc.*, 2003, **126**, 62-63.
69 W. M. Liu, Z. G. Guo and B. L. Su, *Appl. Phys. Lett.*, 2008, **92**, 063104.
70 W. J. Wang, T. C. Lee and T. Y. Han, *J. Adhes. Sci. Technol.*, 2009, **23**, 1799-1810.
71 S. Szunerits, H. Q. Liu, M. Pisarek, W. G. Xu and R. Boukherroub, ACS *Appl. Mater. Interface*, 2009, **1**, 2086-2091.
72 L. Feng, S. Wang and L. Jiang, *Adv. Mater.*, 2006, **18**, 767-770.
73 J. H. Xu, M. Li and Q. H. Lu, *J. Mater. Chem.*, 2007, **17**, 4772-4776.
74 J. M. Lim, W. Y. Zhu and L. I. Jiang, *Macromol. Rapid Comm.*, 2008, **29**, 239-243.
75 J. J. Zhou, P. Jiang, H. F. Fang, C. Y. Wang, Z. L. Wang and S. S. Xie, *Adv. Funct. Mater.*, 2007, **17**, 1303-1310.
76 Z. F. Bian, H .X. Li, J. Zhu, D .Q. Zhang, G. S. Li, Y. N. Huo, H. Li and Y. F. Lu, *J. Am. Chem. Soc.*, 2007, **129**, 8406-8407.
77 V. K. Praveen, S. Srinivasan, R. Philip and A. Ajayaghosh, *Angew. Chem. Int. Ed.*, 2008, **47**, 5750-5754.
78 Z. G. Guo, D. A. Wang, Y. M. Chen, J. C. Hao and W. M. Liu, *Inorg. Chem.*, 2007, **46**, 7707-7709.
79 D. K. Sarkar, A. Safaee and M. Farzaneh, *Appl. Surf. Sci.*, 2008, **254**, 2493-2498.
80 A. Strep, N. Vourdas, A. G. Boudouvis and E. Gogolides, *Microelectron. Eng.*, 2008, **85**, 1124-1127.
81 M. L. Liu and H. C. Shin, *Chem. Mater.*, 2004, **16**, 5460-5464.
82 F. Shi, X. Zhang, X. Yu, H. Liu, Y. Fu, L. Jiang, X. Li and Z. Q. Wang, *J. Am. Chem. Soc.*, 2004, **126**, 3064-3065.
83 Y. Jang, J. T. Han, D. Y. Lee, J. H. Park, S. H. Song and D. Y. Ban, *J. Mater. Chem.*, 2005, **15**, 3089-3092.
84 S. Fujihara, E. Hogono, I. Honma and H. S. Zhou, *J. Am. Chem. Soc.*, 2005, **127**, 13458-13459.
85 S. E. J. Bell, I. A. Larmour and G. C. Saunders, *Angew. Chem. Int. Ed.*, 2007, **46**, 1710-1712.
86 W. Barthlott, R. Furstner, C. Neinhuis and P. Walzel, *Langmuir*, 2005, **21**, 956-961.
87 Y. Chen, M. Callies, F. Marty, A. Pepin, D. Quere, *Microelectron. Eng.*, 2005, **78-79**, 100-105.
88 P. N. B. Barlett, M. E. Abdelsalam and T. Kelf, *Langmuir*, 2005, **21**, 1753-1757.
89 Y. Li, X. J. Huang, S. H. Heo, C. C. Li, Y. K. Choi, W. P. Cai and S. O. Cho, *Langmuir*, 2006, **23**, 2169-2174.
90 Y. Li, C. C. Li, S. O. Cho, G. T. Duan and W. P. Cai, *Langmuir*, 2007, **23**, 9802-9807.
91 W. Cai, Y. Li, B. Cao, G. Duan, F. Sun, C. Li and L. Jia, *Nanotechnology*, 2006, **17**, 238-243.
92 Y. Li, W. Cai, G. Duan, B. Cao, F. Sun and F. Lu, *J. Colloid Interface Sci.*, 2005, **287**, 634-639.
93 Y. Li, G. Duan and W. Cai, *J. Colloid Interface Sci.*, 2007, **314**, 615-620.
94 Y. Li, W. Cai and G. Duan, *J. Adhes. Sci. Technol.*, 2008, **22**, 1949-1965.
95 L. Li, Y. Li, S. Gao and N. Koshizaki, *J. Mater. Chem.*, 2009, **19**, 8366-8371.
96 H. Notsu, W. Kubo, I. Shitanda and T. Tatsuma, *J. Mater. Chem.*, 2005, **15**, 1523-1527.
97 D. Hu, Y. Zhu, M. X. Wang, L. Jiang and Y. Wei, *Adv. Mater.*, 2007, **19**, 2092-2096.
98 J. Tang, Y. Y. Liu, R. H. Wang, H. F. Lu, L. Li, Y. Y. Kong, K. H. Qi and J. H. Xin, *J. Mater. Chem.*, 2007, **17**, 1071-1078.
99 X. G. Hu, T. Wang and S. J. Dong, *Chem. Commun.*, 2007, **18**, 1849-1851.
100 V. Tsyalkovsky, K. Ramaratnam, V. Klep and I. Luzinov, *Chem. Commun.*, 2007, **43**, 4510-4512.
101 Y. Ofir, B. Samanta, P. Arumugam and V. M. Rotello, *Adv. Mater.*, 2007, **19**, 4075-4079.
102 L. Q. Ge, C. Sun and Z. Z. Gu, *Thin Solid Films*, 2007, **515**, 4686-4690.
103 J. A. Orlicki, N. E. Zander, A. S. Karikari, T. E. Long and A. M. Rawlett, *Chem. Mater.*, 2007, **19**, 6145-6149.
104 Y. L. Lee and H. J. Tsai, *Langmuir*, 2007, **23**, 12687-12692.
105 Y. Li, E. J. Lee and S. O. Cho, *J. Phys. Chem. C*, 2007, **111**, 14813-14817.
106 Y. M. Yang, P. S. Szu and Y. L. Lee, *Nanotechnology*, 2007, **18**, 465604.
107 D. Wu, W. Ming, R. Van Benthem and G. de With, *Nano Lett.*, 2005, **5**, 2298-2301.
108 H. Chen, L. B. Zhang, J. Q. Sun and J. C. Shen, *Chem. Mater.*, 2007, **19**, 948-953.
109 F. C. Cebeci, L. Zhai, R. E. Cohen and M. F. Rubner, *Nano Lett.*, 2004, **4**, 1349-1353.

110 M. Ma, Y. Mao, M. Gupta, K. K. Gleaason and G. C. Rutledge, *Macromolecule*, 2005, **38**, 9742-9748.
111 B. K. Tay, X. B. Yan, Y. Yang and Y. K. Po, *J. Phys. Chem. C*, 2007, **111**, 17254-17259.
112 R. Vajtai, L. J. Ci and P. M. Ajayan, *J. Phys. Chem. C*, 2007, **111**, 9077-9080.
113 H. B. Xie, S. H. Li, S. B. Zhang and X. H. Wang, *Chem. Commun.*, 2007, **46**, 4857-4859.
114 S. W. Lam, W. Y. Gan, K. Chiang, R. Amal, H. J. Zhao and M. P. Brungs, *J. Mater. Chem.*, 2007, **17**, 952-954.
115 H. Kono, X. T. Zhang, Z. Y. Liu, S. Nishimoto, D. A. Tryk, T. Murakami, H. Sakai, M. Abe and A. Fujishima, *Chem. Commun.*, 2007, **46**, 4949-4951.
116 Q. H. Wang and W. X. Hou, *Langmuir*, 2007, **23**, 9695-9698.
117 M. Jin, X. T. Zhang, Z. Y .Liu, D. A. Tryk, S. Nishimoto, T. Murakami and A. Fujishima, *J. Phys. Chem. C*, 2007, **111**, 14521-14529.
118 Y. Q. Wen, J. X. Wang, J. P. Hu, Y. L. Song and L. Jiang, *Adv. Funct. Mater.*, 2007, **17**, 219-225.
119 D. Wu, H. F. Hoefnagels, G. With and W. Ming, *Langmuir*, 2007, **23**, 13158-13163.
120 Y. Zhu, Z. B. Huang, J. H. Zhang and G. F. Yin, *J. Phys. Chem. C*, 2007, **111**, 6821-6825.
121 Y. Li,W. Cai and G. Duan, *Chem. Mater.*, 2007, **20**, 615-624.
122 E. Benito, N. Garcia, J. Guzman and Y. Tiemblo, *J. Am. Chem. Soc.*, 2007, **129**, 5052-5069.
123 Y. X. Wang, W. B. Zhong, Y. Yan, Y. F. Sun, J. P. Deng and W. T. Yang, *J. Phys. Chem. B*, **111**, 3918-3926.
124 S. Park, W. K. Cho, S. Y. Jon and S. Choil, *Nanotechnology*, 2007, **18**, 395602.
125 X. F. Wen, A. L. Qu, P. H. Pi, J. Cheng and Z. R. Yang, *Appl. Surf. Sci.*, 2007, **253**, 9430-9434.
126 F. Wang, S. Song and J. Zhang, *Chem. Commun.*, 2009, **28**, 4239-4241.
127 C. T. Hsieh, W. Y. Chen, F. L. Wu and W. M. Hung, *Diamond Relat. Mater.*, 2010, **19**, 26-30.
128 C. K. Saul, E. Burkarter, F. Thomazi, N. C. Cruz, L. S. Roman and W. H .Schreiner, *Surf. Coat. Technol.*, 2007, **202**, 194-198.
129 T. Mizukoshi, H. Matsumoto, M. Minagawa and A. Tanioka, *J. Appl. Polym. Sci.*, 2007, **103**, 3811-3817.
130 J. Liang, Z. G. Guo, J. Fang, B. G. Guo and W. M. Liu, *Adv. Eng. Mater.*, 2007, **9**, 316-321.
131 (a) K. Byrappa and M. Yoshimura: Handbook of Hydrothermal Technology, *Noyes Publications*, William Andrew Publishing LLC, USA, 2001. (b) G. R. Patzke, Y. Zhou, R. Kontic and F. Conrad, *Angew. Chem. Int. Ed.*, 2011, **50**, 826-859.
132 R. Roy, *J. Solid State Chem.*, 1994, **111**, 11-17.
133 S. Somiya: Hydrothermal Reactions for Materials Science and Engineering, An Overview of Research in Japan, *Elsevier Science Publishers Ltd.*,UK,1989,**edition 1.**
134 S. Somiya and R. Roy, *Bull. Mater. Sci.*, 2000, **23(6)**, 453-460.
135 *http://www.alexandrite.net/chapters/chapter7/synt*
136 L. Y. Yeo and J. R. Friend, *J. Exp. Nanosci.*, 2006, **1**, 177-209.
137 G. Taylor, *Proc. R.Soc. London. A*, 1969, **313**, 453-475.
138 L. Cao, A. K. Jones, V. K. Sikka, J. Wu and D. Gao, *Langmuir*, 2009, **25(21),** 12444-12448.
139 R. L. Webb and B. Na, *Int. J. Heat Mass Transfer*, 2003, **46**, 3797-3808.
140 (a) J. A. Taylor, T. N. Krupenkin, T. M. Schneider and S. Yang, *Langmuir*, 2004, **20**, 3824-3827. (b) N. A. Ivanova and A. B. Philipchenko, *Appl. Surf. Sci.*, 2012, **263**, 783-787. (c) M. Shateri-Khalilabad and M. E. Yazdanshenas, *Cellulose*, 2013, **20**, 963–972. (d) L. Wang, G. H. Xi, S. J. Wan, C. H. Zhao and X. D. Liu, *Cellulose*, 2014, DOI: 10.1007/s10570-014-0275-6. (e) Q. Zhu and Q. Pan, *ACS Nano*, 2014, **8**, 1402-1409.
141 A. L. Linsebigler, G. Lu and J. T. Yates, *Chem. Rev.*, 1995, **95** ,735-758.
142 A. Mills, A. Lepre, N. Elliot, S. Bhopal, I. P. Parkin and S. A. O'Neill, *J. Photochem. Photobiol A. Chem.*, 2003, **160**, 213-224.
143 A. Hagfeldtt and M. Gratzel, *Chem. Rev.*, 1995, **95**, 49-68.
144 a) A. Mills and S. Le Hunte, *J. Photochem. Photobiol A. Chem.*, 1997, **108**, 1-35.
b) *https://www.alcoa.com/ecoclean/*
145 a) S. Kim, H. Park and W. Choi, *J. Phys. Chem. B*, 2004, **108**, 6402-6411.
b) *http://www.titanshield.co.il/pdf/E/TS-SolarCoat_V1_E.pdf*
146 A. Lafuma, D. Quere, *Nat. Mater.*, 2003, **2**,457-460.
147 J. Genzer and A. Marmur, *MRS Bull.*, 2008, **33**, 742-746.
148 B. Bhusan, Y. C. Jung and K. Koch, *Philos. Trans. R.Soc. A.*, 2009, **367**, 1631-1672.
149 X. Zhang, F. Shi, J. Niu, Y. G. Jiang, Z. Q. Wang, *J. Mater. Chem.*, 2008, **18**, 621-633.
150 X. Yao, Y. Song and L. Jiang, *Adv. Mater.*, 2011, **23(6),** 719-734.
151 M. J. Xu, N. Lu, H .B. Xu, D. P. Qi, Y. D. Wang, S. L. Shi and L. F. Chi, *Soft Matter*, 2010, **6**, 1438-1443.
152 H. Y. Erbil, A. L. Denirel, Y. Avci and O. Mert, *Science*, 2003, **299**, 1377-1380.
153 L. Jiang, Y. Zhao and J. Zhai, *Angew. Chem. Int. Ed.*, 2004, **43**, 4338-4341.
154 L. Feng, S. H. Li, Y. S. Li, H. J. Li, L. J. Zhang, J. Zhai, Y. L .Song, B. Q. Liu, L. Jiang and D. B. Zhu, *Adv. Mater.*, 2002, **14**, 1857-1860.
155 W. J. Zhao, L. P. Wang and Q. J. Xue, *J. Phys. Chem. C*, 2010, **114**, 11509-11514.
156 J. Gao, Y. L. Liu, H. P. Xu, Z. Q. Wang and X. Zhang, *Langmuir*, 2009, **25**, 4365-4369.
157 J. A. Gao, Y. L. Liu, H. P. Xu, Z. Q. Wang and X. Zhang, *Langmuir*, 2010, **26**, 9673-9676.
158 S. Z. Wu, D. Wu, J. Yao, Q. D. Chen, J. N. Wang, L. G. Niu, H. H. Fang and H. B. Sun, *Langmuir*, 2010, **26**, 12012-12016.
159 P. Vukusic and J. R. Sanbles, *Nature*, 2003, **424**, 852-855.
160 S. Kinoshita and S. Yoshioka, *Chem Phy Chem*, 2005, **6**, 1442-1459.
161 A. L .Ingram and A. R. Parker, *Philos. Trans. R.Soc. B*, 2008, **363**, 2465-2480.
162 A. R. Parker, *Philos. Trans. R.Soc. A*, 2009, **367**, 1759-1782.
163 O. Sato, S. Kubo and Z. Z. Gu, *Acc. Chem. Res.*, 2009, **42**, 1-10.
164 Y. M. Zhang, X. F. Ghao and L. Jiang, *Soft Matter*, 2007, 3, 178-182.
165 Z. Z. Gu, H. Uetsuka, K. Takahashi, R. Nakajima, H. Onishi, A. Fujishima and O. Sato, *Angew. Chem. Int. Ed.*, 2003, **42**, 894-897.
166 J. Y. Huang, X. D. Wang and Z. L. Wang, *Nano Lett.*, 2006, **6**, 2325-2331.

167 J. Zi, X. D. Yu, Y. Z. Li, X. H. Hu ,C. Xu, X. J. Wang, X. H. Liu and R. T. Fu, *Proc. Natl. Acad. Sci. USA.*, 2003, **100**, 12576-12578.
168 S. Kinoshita, S. Yoshioka and K. Kawagoe, *Proc. R.Soc. Lond. B.*, 2002, **269**, 1417-1421.
169 D. L. Hu, B. Chan, J. W. M. Bush, *Nature*, 2003, **424**, 663-666.
170 X. F. Gao and L. Jiang, *Nature*, 2004, **432**, 36-136.
171 X. Yao, Q. W. Chen, L. Xu, Q. K. Li, Y. L. Song, X. F. Gao, D. Quere and L. Jiang, *Adv. Funct. Mater.*, 2010, **20**, 656-662.
172 Y. F. Li, J. H. Zhang and B. Yang, *Nano Today*, 2010, **5**, 117-127.
173 M. Srinivasarao, *Chem. Rev.*, 1999, **99**, 1935-1961.
174 A. R. Parker and H. E. Townley, *Nat. Nanotechnol.*, 2007, **2**, 347-353.
175 W. H. Miller, G. D. Bernard, J. L. Allen, *Science*, 1968, **162**,760-767.
176 D. G. Stavenga, S. Foletti, G. Palasantzas and K. Arikawa, *Proc. R.Soc. Lond. B*, 2006, **273**, 661-667.
177 G. S. Watson and J. A. Watson, *Appl. Surf. Sci.*, 2004, **235**, 139-144.
178 J. Y. Huang, X. D. Wang and Z. L. Wang, *Nanotechnology*, 2008, **19**, 025602.
179 Y. F. Huang, S. Chattopadhyay, Y. J. Jen, C. Y. Peng, T. A. Liu, Y. K. Hsu, C. L. Pan, H. C. Lo, C. H. Hsu, Y. H. Chang, C. S. Lee, K. H. Chen and L. C. Chen, *Nat. Nanotechnol.*, 2007, **2**, 770-774.
180 Y. F. Li, J. H. Zhang, S. J. Zhu, H. P. Dong, Z. H. Wang, Z. Q. Sun, J. R. Guo, B. Yang, *J. Mater. Chem.*, 2009, **19**, 1806-1810.
181 X. F. Gao, X. Yan, X. Yao, L. Xu, K. Zhang, J. H. Zhang, B. Yang, L. Jiang, *Adv. Mater.*, 2007, **19**, 2213-2217.
182 W. Lee, M. K. Jin, W. C. Yoo and J. K. Lee, *Langmuir*, 2004, **20**, 7665-7669.
183 G. M. Zhang, J. Zhang, G. Y. Xie, Z. F. Liu, H. B. Shao, *Small*, 2006, **2**, 1440-1443.
184 G. Y. Xie, G. M. Zhang, F. Lin, J. Zhang, Z. F. Liu and S. C. Mu, *Nanotechnology*, 2008, **19**, 095605.
185 C. H. Sun, A. Gonzalez, N. C. Linn, P. Jiang and B. Jiang, *Appl. Phys. Lett.*, 2008, **92**, 051107.
186 W. L. Min, B. Jiang and P. Jiang, *Adv. Mater.*, 2008, 20, 3914-3918.
187 Kesong Liu and Lei Jiang, *Nano Today*, 2011, **6**, 155-175.
188 W. Choi, A. Tuteja, S. Chhatre, J. M. Mabry, R. E. Cohen, G. H. McKinley, *Adv. Mater.*, 2009, **21(21)**, 2190-2195.
189 Y. C. Jung and B. Bhushan, *Langmuir*, 2009, **25(24)**, 14165-14173.
190 D. Wang, X. Wang, X. Liu and F. Zhou, *J. Phys. Chem. C*, 2010, **114(21)**, 9938-9944.
191 C. Aulin, J. Netrval, L. Wagberg and T. Lindstrom, *Soft Matter*, 2010, **6**, 3298-3305.
192 S. S. Chhatre, A. Tuteja, W. Choi, A. Revaux, D. Smith, J. M. Mabry, G. H. McKinley and R. E. Cohen, *Langmuir*, 2009, **25(23)**, 13625-13632.
193 Y. Liu, Y. Xiu, D. W. Hess and C. P. Wong, *Langmuir*, 2010, **26(11)**, 8908-8913.
194 H. Bellanger, T. Darmanin, E. T. de Givenchy and F. Guittard, *J. Mater. Chem. A*, 2013, **1**, 2896-2903.
195 F. Dong and C. S. Ha, *Macromol. Res.*, 2011, **19(2)**, 101-104.
196 a) M. Uyanik, E. Arpac, H.Schmidt, M.Akarsu, F.Sayilkan and H. Sayilkan, *J. Appl. Polym. Sci.*, 2006, **100(3)**, 2386-2392.
b) Xi Yao, Jun Gao, Yanlin Song and Lei Jiang, *Adv. Funct. Mater.*, 2011, **21(22)**, 4270-4276.
197 a) A. Steele, I. Bayer and E. Loth, *Nano Lett.*, 2009, **9(1)**, 501-505.
b) A. Tuteja, W. Choi, M. Ma, J. M. Mabry, S. A. Mazzella, G. C. Rutledge, G. H. McKinley, R. E. Cohen, *Science*, 2007, **318**, 1618-1622.
198 a) J. Zhang and S. Seeger, *Angew. Chem. Int. Ed.*, 2011, **50(29)**, 6652-6656. b) V. A. Ganesh, S. S. Dinachali, A. S. Nair and S. Ramakrishna, *ACS Appl. Mater. Interfaces*, 2013, **5**, 1527-1532. (c) L. Li, Y. Wang, C. Gallaschun, T. Risch and J. Sun, *J. Mater. Chem.*, 2012, **22**, 16719. (d) Z. Cheng, H. Lai, Y. Du, K. Fu, R. Hou, N. Zhang and K. Sun, *ACS Appl. Mater. Interfaces*, 2013, **5**, 11363-11370.
199 S. E. Lee, H. J. Kim, S. H. Lee and D. G. Choi, *Langmuir*, 2013, **29**, 8070-8075.
200 D. Xiong, G. Liu, E. J. Scott Duncan, *Polymer.*, 2013, **54(12)**, 3008-3016.
201 S. Nagappan, J. J. Park, S. S. Park, S. H. Hong, Y. Sik Jeong, W. Ki Lee and C. S. Ha, *Second – Japan - Korea Joint Symposium on Polymer Nanohybrid Mater.2.*, 2013, **20(1)**.
202 Y. C. Sheen, Y. C. Huang, C. S. Liao, H. Y. Chou, F. C. Chang, *J. Polym. Sci., Part B: Polym. Phys.*, 2008, **46(18)**, 1984-1990.
203 C. F. Wang, S. F. Chiou, F. H. Ko, C. T. Chou, H. C. Lin, C. F. Huang and F. C. Chang, *Macromol. Rapid Commun.*, 2006, **27(5)**, 333-337.
204 M. Guo, B. Ding, X. Li, X. Wang, J. Yu and M. Wang, *J. Phys. Chem. C*, 2010, **114(2)**, 916-921.
205 G. R. Choi, J. Park, J. W. Ha, W. D. Kim, H. Lim, *Macromol. Mater. Eng.*, 2010, **295(11)**, 995-1002.
206 E. Yoshida, *Colloid. Polym. Sci.*, 2012, **290(6)**, 525-530.
207 a) X. Deng, L. Mammen, H. J. Butt and D. Vollmer, *Science*, 2012, **335**, 67-70.
b) S. Barthwal, Y. S. Kim and S. H. Lim, *J. Colloid Interface Sci.*, 2013, **400**, 123-129.
208 C. Y. Mou, W. L. Yuan and C. H. Shih, *Thin Solid Films*, 2013, **537**, 202-207.
209 a) V. A. Ganesh, S. S. Dinachali, H. K. Raut, T. M. Walsh, A.S. Nair and S. Ramakrishna, *RSC Adv.*, 2013, **3**, 3819-3824.
b) S. Barthwal, Y. S. Kim and S. H. Lim, *Langmuir*, 2013, **29(38)**, 11966-11974. (c) J. Wang, A. Raza, Y. Si, L. Cui, J. Ge, B. Ding and J. Yu, *Nanoscale*, 2012, **4**, 7549.
210 H. Lee, S. M. Dellatore, W. M. Miller, P. B. Messersmith, *Science*, 2007, **318**, 426-430.
211 Q. Wei, F. Zhang, J. Li, B. Li and C. Zhao, *Polym. Chem.*, 2010, **1**, 1430-1433.
212 C. H. Sun, A. Gonzalez, N. C. Linn, P. Jiang and B. Jiang, *Appl. Phys. Lett.*, 2008, **92**, 051107.
213 N. Dingremont, E. Bergmann, P. Collignon, H. Michael, *Surf. Coat. Technol.*, 1995, **72(3)**, 163-168.
214 X. Hu and J. Ji, *Langmuir*, 2010, **26(4)**, 2624-2629.
215 F. C. Cebeci, Z. Wu, L. Zhai, R. E. Cohen and M. F. Rubner, *Langmuir*, 2006, **22(6)**, 2856-2862.
216 W. Yuan, J. Ji, J. Fu, J. Shen, *J. Biomed. Mater. Res. Part B Appl. Biomater.*, 2008, **85B(2)**, 556-563.
217 N. N. Voevodin, V. N. Balbyshev, M. Khobaib, M. S. Donley, *Prog. Org. Coat.*, 2003, **47(3-4)**, 416-423.
218 P. Jin, G. Xu, M. Tazawa and K. Yoshimura, *Jpn. J. Appl. Physics*, 2002, **41**, L278-L280.
219 Xiujian Zhao, Qingnan Zhao, Jiaguo Yu, Baoshun Liu, *J. Non-Cryst. Solids*, 2008, **354(12-13)**, 1424-1430.

220 J. Lauridsen, P. Eklund, T. Joelsson, H. Ljungcrantz, A. Oberg, E. Lewin, U. Jansson, M. Beckers, H. Hogberg and L. Hultman, *Surf. Coat. Technol.*, 2010, **205(2)**, 299-305

221 E. S. Ates, H. E. Unalan, *Thin Solid Films*, 2012, **520(14)**, 4658-4661.

222 H. Schmidt, *J. Non-Cryst. Solids*, 1994, **178**, 302-312.

223 H. Li, Y. Chen, C. Ruan, W. Gao and Y. Xie, *J. Nanopart. Res.*, 2001, **3(2-3)**, 157-160.

224 E. Dervishi, Z. Li, V. Saini, R. Sharma, Y. Xu, M. K. Mazumder, A. S. Biris, S. Trigwell, A. R. Biris, D. Lupu, & D. Saini, *IEEE Trans. Ind. Appl.*, 2009, **45(5)**, 1547-1552.

225 M. Faustini, L. Nicole, C. Boissiere, P. Innocenzi, C. Sanchez and D. Grosso, *Chem. Mater.*, 2010, **22(15)**, 4406-4413.

226 L. Miao, L. F. Su, S. Tanemura, C. A. J. Fisher, L. L. Zhao, Q. Liang and G. Xu, *Appl. Energy*, 2013, **112**, 1198-1205.

227 R. Prado, G. Beobide, A. Marcaide, J. Goikoetxea and A. Aranzabe, *Sol. Energy Mater. Sol. Cells*, 2010, **94**, 1081-1088.

228 J. Son, S. Kundu, L. K.Verma, M. Sakhuja, A. J. Danner, C. S. Bhatia and H. Yang, *Sol. Energy Mater. Sol. Cells*, 2012, **98**, 46-51.

229 L. K. Verma , M. Sakhuja , J. Son , A. J. Danner , H. Yang , H. C. Zeng and C. S. Bhatia, *Renewable Energy*, 2011, **36**, 2489-2493.

230 (a) Z. Liu, X. Zhang, T. Murakami and A. Fujishima, *Sol. Energy Mater. Sol. Cells*, 2008, **92**, 1434-1438. (b) X. Tang, Y. Si, J. Ge, B. Ding, L. Liu, G. Zheng, W. Luo and J. Yu, *Nanoscale*, 2013, **5**, 11657.

231 (a) K. Liu, Y. Tian and L. Jiang, *Prog. Mater Sci.*, 2013, **58**, 503-564. (b) J. Yang, Z. Z. Zhang, X. H. Xu, X. T. Zhu, X. H. Men, and X. Y. Zhou, *J. Mater. Chem.*, 2012, **22**, 2834-2837.

232 (a) H. Sawada, Y. Ikematsu, T. Kawase, and Y. Hayakawa, *Langmuir*, 1996, **12**, 3529-3530. (b) K. Sasazawa, J. Kurachi, T. Narumi, H. Nishi, Y. Yamamoto, and H. Sawada, *J. Appl. Polym. Sci.*, 2007, **103**, 110-117. (c) J. A. Howarter, and J. P. Youngblood, *Adv. Mater.*, 2007, **19**, 3838-3843. (d)) J. A. Howarter, and J. P. Youngblood, *Macromol. Rapid Commun.*, 2008, **29**, 455-466.

233 (a) K. S. Liu and L. Jiang, *Nanoscale*, 2011, **3**, 825–838. (b) L. Feng, Z. Y. Zhang, Z. H. Mai, Y. M. Ma, B. Q. Liu, and L. Jiang, *Angew. Chem. Int. Ed.*, 2004, **43**, 2012–2014. (c) M. Guix, J. Orozco, M. Garcia, W. Gao, S. Sattayasamitsathit, and A. Merkoci, *ACS Nano*, 2012, **6**, 4445–4451.

234 (a) Z. X. Xue, S. T. Wang, L. Lin, L. Chen, M. J. Liu, L. Feng, *Adv Mater.*, 2011, **23**, 4270–4273. (b) L. B. Zhang, Z. H. Zhang, and P. Wang, *NPG Asia Mater*, 2012, **4**, e8. (c) D. Tian, X. Zhang, Y. Tian, Y. Wu, X. Wang, and J. Zhai, *J. Mater. Chem.*, 2012, **22**, 19652–19657.

235 X. Zhang, Z. Li, K. Liu and L. Jiang, *Adv. Funct. Mater.*, 2013, **23**, 2881–2886.

236 Y. Shang, Y. Si, A. Raza, L. Yang, X. Mao, B. Ding and J. Yu, *Nanoscale*, 2012, **4**, 7847.

237 Q. Wen, J. Di, L. Jiang, J. Yu and R. Xu, *Chem. Sci.*, 2013, **4**, 591.

238 L. Zhang, Y. Li, J. Sun, and J. Shen, *Langmuir*, 2008, **24**, 10851-10857.

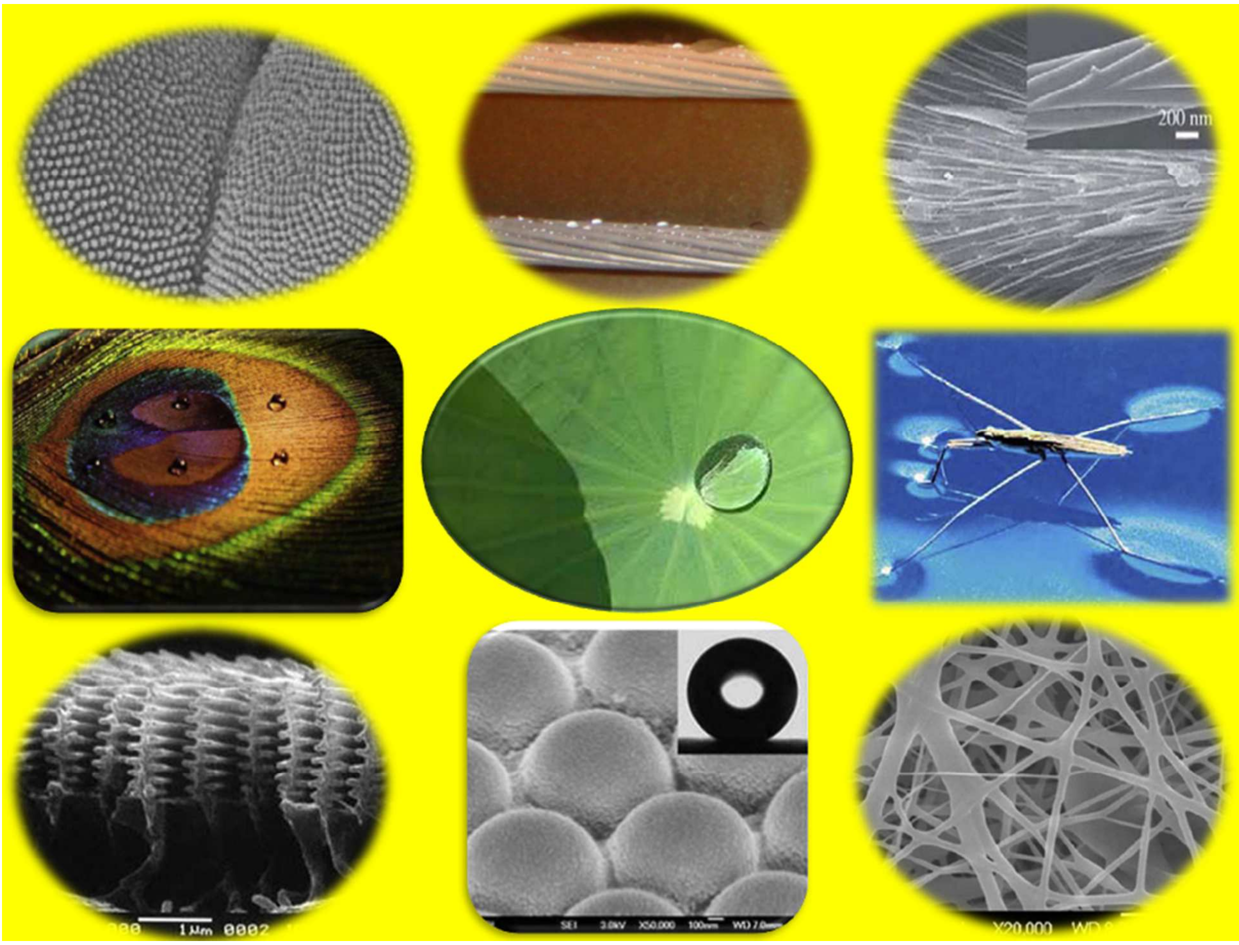

Self-cleaning and multifunctional materials find immense applications in windows, solar panels, cements, paints, textiles, etc. This state-of-the-art review summarizes the materials involved in self-cleaning and multifunctional coatings.